UNIVERSITYOF BIRMINGHAM

Generation of liposomes to study the effect of mycobacterium tuberculosis lipids on HIV-1 cis- and trans-infections

Pouget, Marion; Coussens, Anna K; Ruggiero, Alessandra; Koch, Anastasia; Thomas, Jordan; Besra, Gurdyal S; Wilkinson, Robert J; Bhatt, Apoorva; Pollakis, Georgios; Paxton, William A

[Link to publication on Research at Birmingham portal](#)

Article

Generation of Liposomes to Study the Effect of *Mycobacterium Tuberculosis* Lipids on HIV-1 *cis-* and *trans*-Infections

Marion Pouget [1,2], Anna K. Coussens [3,4], Alessandra Ruggiero [1,5], Anastasia Koch [3], Jordan Thomas [1], Gurdyal S. Besra [6], Robert J. Wilkinson [3,7,8], Apoorva Bhatt [6], Georgios Pollakis [1,*] and William A. Paxton [1,*]

1   Department of Clinical Infection, Microbiology and Immunology, Institute of Infection, Veterinary and Ecological Sciences, University of Liverpool, Liverpool L69 7BE, UK; marion.pouget@ucd.ie (M.P.); aler@liverpool.ac.uk (A.R.); hljthom2@liverpool.ac.uk (J.T.)
2   UCD Centre for Experimental Pathogen Host Research, University College Dublin, Belfield, Dublin 4, Ireland
3   Wellcome Center for Infectious Diseases Research in Africa, Institute of Infectious Disease and Molecular Medicine and Department of Medicine, University of Cape Town, Observatory, Cape Town 7925, South Africa; coussens.a@wehi.edu.au (A.K.C.); a.koch@uct.ac.za (A.K.); robert.wilkinson@uct.ac.za (R.J.W.)
4   Walter and Eliza Hall Institute of Medical Research, Parkville 3279, Australia
5   Academic Department of Pediatrics (DPUO), IRCCS Ospedale Pediatrico Bambino Gesù, Piazza S. Onofrio 4, 00165 Rome, Italy
6   Institute of Microbiology and Infection and School of Biosciences, University of Birmingham, Birmingham B15 2TT, UK; g.besra@bham.ac.uk (G.S.B.); a.bhatt@bham.ac.uk (A.B.)
7   Department of Infectious Diseases, Imperial College, London W2 1PG, UK
8   The Francis Crick Institute, London NW1 1AT, UK
*   Correspondence: g.pollakis@liverpool.ac.uk (G.P.); W.A.Paxton@liverpool.ac.uk (W.A.P.); Tel.: +44-151-795-9681 (G.P.); +44-151-795-9605 (W.A.P.)

Abstract: Tuberculosis (TB) is the leading cause of death among HIV-1-infected individuals and *Mycobacterium tuberculosis* (*Mtb*) co-infection is an early precipitate to AIDS. We aimed to determine whether *Mtb* strains differentially modulate cellular susceptibility to HIV-1 infection (*cis-* and *trans*-infection), via surface receptor interaction by their cell envelope lipids. Total lipids from pathogenic (lineage 4 *Mtb* H37Rv, CDC1551 and lineage 2 *Mtb* HN878, EU127) and non-pathogenic (*Mycobacterium bovis* BCG and *Mycobacterium smegmatis*) *Mycobacterium* strains were integrated into liposomes mimicking the lipid distribution and antigen accessibility of the mycobacterial cell wall. The resulting liposomes were tested for modulating in vitro HIV-1 *cis-* and *trans*-infection of TZM-bl cells using single-cycle infectious virus particles. *Mtb* glycolipids did not affect HIV-1 direct infection however, *trans*-infection of both R5 and X4 tropic HIV-1 strains were impaired in the presence of glycolipids from *M. bovis*, *Mtb* H37Rv and *Mtb* EU127 strains when using Raji-DC-SIGN cells or immature and mature dendritic cells (DCs) to capture virus. SL1, PDIM and TDM lipids were identified to be involved in DC-SIGN recognition and impairment of HIV-1 *trans*-infection. These findings indicate that variant strains of *Mtb* have differential effect on HIV-1 *trans*-infection with the potential to influence HIV-1 disease course in co-infected individuals.

Keywords: HIV-1; TB; *Mycobacterium tuberculosis*; in vitro; DC-SIGN; liposomes; *trans*-infection; SL1; TDM; PDIM; H37Rv; HN878; CDC1551; EU127; BCG; *M. smegmatis*

1. Introduction

Human immunodeficiency virus type 1 (HIV-1) and *Mycobacterium tuberculosis* (*Mtb*) co-infection results in a loss of numerous immunological functions and ultimately leads to death when not treated. The WHO estimated in 2019 that 208,000 people died of HIV-associated tuberculosis [1]. Both, *Mtb* and HIV-1 can induce profound changes in the host immune response resulting in increased rates of active *Mtb* disease or the exacerbation

of HIV-1 infection. *Mtb* creates a favorable environment for HIV-1 direct infection (*cis*-infection) and/or replication, as *Mtb* infection leads to the activation and induction of immune responses [2–4].

Due to the glycosylation of the mycobacterial cell wall and HIV-1 envelope protein gp120, both pathogens engage C-type lectin receptors [5]. In the case of HIV-1, numerous cells of the immune system, including dendritic cells, can bind and capture HIV-1 via an array of C-type lectins expressed on the cell surface. Binding not only promotes the capture, processing and subsequent presentation of HIV-1 antigen to other cells of the immune system but can result in the capture and transfer of HIV-1 virions to susceptible cells, a mechanism termed *trans*-infection [6–9]. Different receptors have been described to be involved with *trans*-infection, such as the mannose receptor MR [6,10,11] and the C-type lectin receptor DC-SIGN [12–15], alongside Siglec via interactions with ganglioside GM3 localised on the virus membrane [16–20].

The mycobacterial cell envelope is complex and composed of carbohydrate polymers such as arabinogalactan (AG) and distinct lipids including mycolic acids (MA) linked to peptidoglycans (PG) and free lipids trehalose dimycolate (TDM), phthiocerol dimy-cocerosate (PDIM/DIM), sulfolipids (SLs), phosphatidylinositol mannosides (PIM), lipo-mannan (LM) and lipoarabinomannan (LAM) [21–26]. These outer envelope lipids play an important role in structural integrity and can modulate the host immune response, therefore influencing *Mycobacterium* pathogenicity. MA constitutes a natural barrier of the bacteria and the nature of its composition and oxygenation can influence *Mtb* pathogenicity [27,28] by modulation of macrophage activation and differentiation [29,30]. In addition, the inflammatory response can be associated with AG and PG structures [31]. TDM (also known as cord factor) is a major contributor to inflammation [32–35] and can also modulate macrophage activation [32,36,37], macrophage surface markers expression [38] and granuloma formation [39,40]. SLs are sulphated trehalose esters and several studies using *Mtb* mutants in SL1 biosynthesis have revealed its role in *Mtb* virulence, for example, mmpL8 knock-out mutants of *Mtb* have been shown to attenuate bacterial virulence in mouse models [41,42]. PDIMs have been described to play a role in *Mtb* virulence [43,44] and the presence of PDIMs at the bacterial surface can aide escape from macrophage recognition [45,46], mask pathogen associated molecular patterns (PAMPs) [47], and prevent macrophage recruitment [48]. PIMs are glycoconjugates and represent the major components of the mycobacterial cell envelope and are precursors of LM, LAM and mannan capped lipoarabinomannan (ManLAM). Mannoside caps associated to PIMs can be recognised by phagocytic receptors such as C-type lectins, including MR and DC-SIGN [49–51]. Additionally, LM has been described as a TLR2 and TLR4 ligand, modulating anti- and pro-inflammatory responses against the bacteria [52–56].

The proportion of lipids present within the mycobacterial cell wall can vary between *Mycobacterium* strains resulting in different biochemical properties [57,58]. Variation in lipid compositions inside *Mtb* species can impact on their pathogenicity. Different clinical *Mtb* strains are associated with important disparities in immune response activation such as CDC1551 and HN878 [59–62]. Compared to the lineage 4 CDC1551, the lineage 2 Beijing strain HN878 induces an altered immune response partly due to its expression of phenolic glycolipids (PGL), increasing its virulence [63–66]. In order to measure and compare the impact of glycolipids derived from different *Mycobacterium* strains on HIV-1 *cis*- and *trans*-infection, we developed liposomes which contained *Mycobacterium* total lipid extracts from lineage 4 *Mtb* H37Rv, and CDC1551, lineage 2 *Mtb* HN878 and non-pathogenic *M. bovis* BCG and *M. smegmatis*. These liposomes are artificial vesicles composed of a mix of phosphatidylcholine (PC) and cholesterol (Ch) and used as the experimental foundation in our assays. In many cases, liposomes have been used as a carrier for various applications in pharmacology, including for diagnostic purposes, therapeutic treatments of cancer and for use in vaccine technologies [67]. In the context of TB, the interest in using liposomes for vaccination strategies is important and well described in the literature [68–73].

2. Results

2.1. Production of Liposomes Containing Mycobacterium Total Lipids

The initial aim was to identify whether we could incorporate lipid extract antigens from variant *Mycobacterium* strains into liposomes. Unilamellar liposomes were generated with total lipid extracts from differing strains as described. We characterised 0.8PC:0.2Ch, *M. bovis* and *Mtb* H37Rv liposomes generated by NanoSight technology (Figure 1) and Thin-layer chromatography TLC (Figure 2).

A. 0.8PC:0.2Ch 100nm

Mean Size 140.8nm
Concentration 2.08×10^{12} particles/ml

B. 0.8PC:0.2Ch 200nm

Mean Size 182.9nm
Concentration 1.33×10^{12} particles/ml

C. 0.8PC:0.2Ch

Mean Size 171.4nm
Concentration 6.69×10^{11} particles/ml

D. *M. bovis*, BCG (1)

Mean Size 221.3nm
Concentration 1.11×10^{12} particles/ml

E. *M. bovis*, BCG (2)

Mean Size 229.9nm
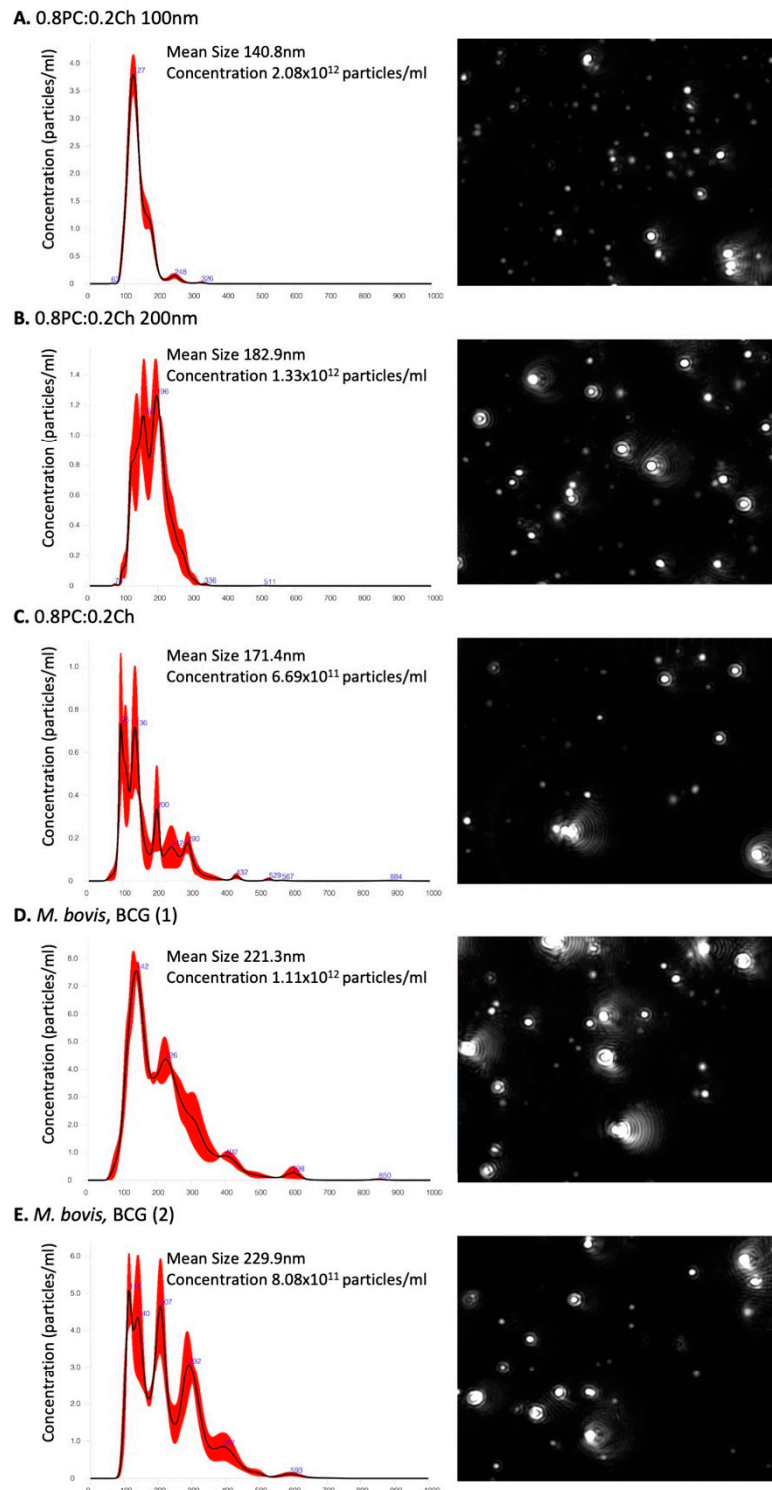Concentration 8.08×10^{11} particles/ml
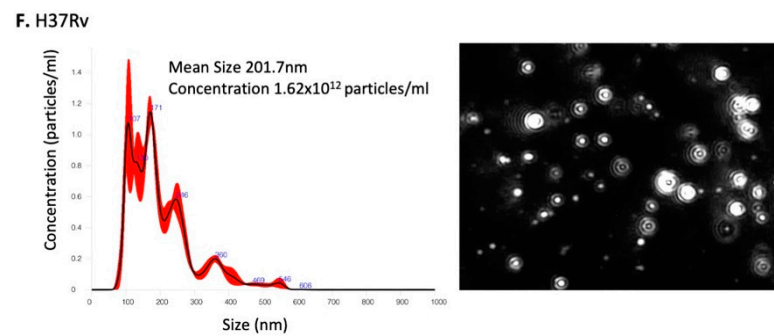
Figure 1. *Cont.*

Figure 1. Liposome-size analysis by NanoSight particle tracking. (**A**) Liposomes generated with the Extruder system at 100 nm size, (**B**) Liposomes generated with the Extruder system at 200 nm size (**C**) 0.8PC:0.2Ch, (**D**) BCG batch n° 1, (**E**) BCG batch n° 2 and (**F**) H37Rv liposomes made by sonication without the Extruder step. Liposome suspensions were diluted 1:1000–1:2000 in PBS, and three 60 s videos were recorded. The data shown are from one experiment. On the right are graphs showing the results of particle concentration and their size measurement; and on the left are liposomes observed at the screen shot from NTA video.
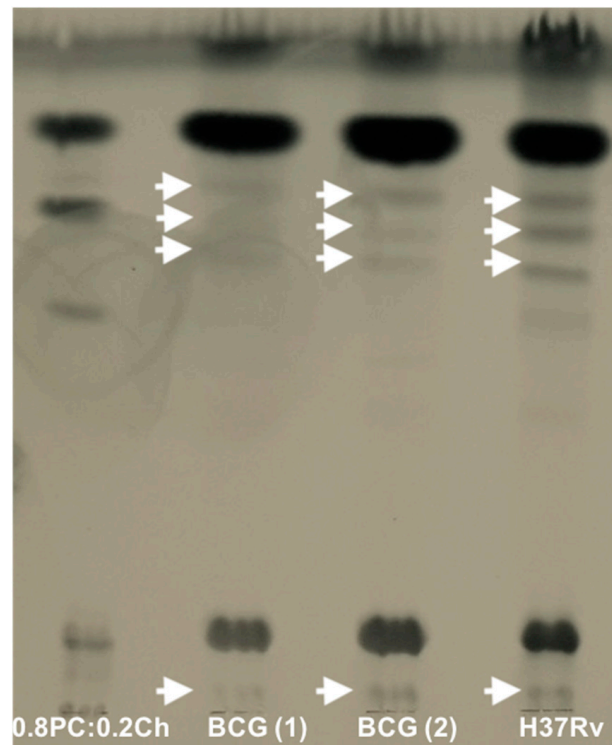
Figure 2. Thin-layer chromatography (TLC) analyses of 0.8PC:0.2Ch, BCG and H37Rv liposomes. 10 µL of liposomes solution made in water were spotted and dried on a silica gel 60 F254 plate. Separation occurred in 60:16:2 CHCl$_3$:MeOH:H$_2$O solvent and was visualised by staining with molybdophosphoric acid and charring. The arrows show the presence of lipids from mycobacterial origin. The data are from one representative experiment.

Visualisation of liposome particles using NanoSight NS300 optics and software was used to define their size and distribution (Figure 1). Calibrated liposomes were generated with an additional step of extrusion following sonication, producing: 0.8PC:0.2Ch liposomes at 100 nm (Figure 1A) and 200 nm (Figure 1B), respectively. In parallel, 0.8PC:0.2Ch liposomes were produced with a step of sonication only with no calibration (Figure 1C). Two separate batches of *M. bovis* liposomes were generated (Figure 1D,E) and each measured on average 221.3 and 229 nm, respectively, while the mean size of H37Rv liposomes

(Figure 1F) was 201.7 nm. The similar sizes and distribution of the two independent preparations of *M. bovis* liposomes demonstrates the reproducibility of the liposome generation technique. Due to a single sonication step, the population of *M. bovis* and H37Rv liposomes generated is heterogenous compared to calibrated liposomes at 100 nm and 200 nm. Additionally, *Mycobacterium* liposomes appear larger than the calibrated liposomes [0.8PC:0.2Ch 100 nm (140.8 nm), 0.8PC:0.2Ch 200 nm (182.9 nm)] and 0.8PC:0.2Ch liposomes generated with a single sonication step (171.4 nm, Figure 1C). This size variation is likely explained by the incorporation of the *Mycobacterium* lipids onto *M. bovis* and H37Rv liposomes. When comparing particle concentrations, we observed similar order values between liposome preparations included between $0.6 - 2 \times 10^{12}$ particles per ml. A TLC analysis of lipids extracted from the liposomes revealed two sets of lipid species. The first set was found in all preparations including the 'empty' liposomes and were thus liposome derived (PC and Ch, shown). The other set of lipid species (shown by arrows) were of relatively lower proportions and were only found in liposomes that were reconstituted with mycobacterial lipids and thus were of mycobacterial origin (Figure 2). However, between *M. bovis* and H37Rv we observed variation in the intensity of the lipid bands, suggesting differences in lipid proportions contained in the liposomes. The analysis, therefore, demonstrates the integration of specific *Mycobacterium* lipids into liposomes.

2.2. Mycobacterium Lipids Do Not Affect HIV-1 Cis-Infection

In order to measure the direct impact of *Mtb* liposomes on HIV-1 *cis*-infection (direct infection), a non-productive HIV-1 pseudo-typed viral particle system (single round of infection) was used in vitro. This system facilitates investigation into interaction or interference of HIV-1 entry and infection via the co-receptors CCR5 and CXCR4 in the presence of *Mycobacterium* derived liposomes. To this end, two types of HIV-1 pseudo-typed viruses were produced, expressing either HIV-1 LAI envelope (HIV-1 X4, utilisng CXCR4) or HIV-1 BAL envelope (HIV-1 R5, utilising CCR5).

The impact of 0.8PC:0.2Ch liposomes (containing PC and cholesterol only) on the viability of the target cells used in this in vitro system (TZM-bl) were tested (Figure S1). Control liposomes composed of a mix of PC and Ch did not affect TZM-bl viability after 48 h of incubation. Additionally, we observed that 0.8PC:0.2Ch liposomes did not interfere with HIV-1 *cis*-infection compared to other liposomes compositions (Figure S2). For these reasons, liposome produced in the ratio 0.6PC:0.2Ch:0.2*Mycobacterium* were chosen to build liposomes incorporating *Mycobacterium* total lipid extracts.

The influence of *Mycobacterium* liposomes containing *M. bovis*, *M. smegmatis*, *Mtb* H37Rv, HN878, CDC1551 and EU127 glycolipids was then assessed for modulating *cis*-infection of TZM-bl cells using HIV-1 X4 and HIV-1 R5 viruses (Figure 3). Two conditions were tested, where liposomes were added to cells at the same time as virus and where liposomes were incubated with cells 30 min prior to infection. In order to compare results from separate experiments, the raw relative light units (RLU) produced on every plate were normalised to the average value of the negative control. For both viruses, in comparison with TZM-bl *cis*-infection in the presence of 0.2PC:0.8Ch liposomes, we did not observe any significant impact of *Mtb* liposomes under the two conditions, suggesting that the tested glycolipids did not have the capacity to interfere with HIV-1 cell attachment and cell entry via co-receptor recognition. Our results indicate that the derived liposomes described do not alter HIV-1 direct infection of TZM-bl cells.

2.3. M. bovis, Mtb H37Rv and EU127 Lipids Interfere with HIV-1 Trans-Infection Mediated by DC-SIGN

We next investigated the influence of *Mtb* lipids on HIV-1 *trans*-infection via binding the DC-SIGN receptor using the same in vitro system of pseudo-typed virus particles that allows a single-round of infection. In this assay, Raji-DC-SIGN cell lines were used to support capture-transfer of HIV-1 R5 or X4 virions due to their expression of DC-SIGN receptor and inability to be infected by the virus through lack of CD4 receptor expression. *Mycobacterial* liposomes were pre-incubated with Raji-DC-SIGN before HIV-1

X4 (Figure 4A) and HIV-1 R5 (Figure 4B) capture. The efficacy of capture-transfer of HIV-1 was normalised to the value of *trans*-infection in the presence of liposomes 0.8PC:0.2Ch (negative control). We observed a strong inhibition of the efficacy of HIV-1 X4 and R5 *trans*-infection mediated by DC-SIGN receptor in the presence of *M. bovis*, *Mtb* H37Rv and EU127 liposomes. Indeed, the non-pathogenic mycobacterial strain *M. bovis* inhibited HIV-1 capture-transfer by 2.4-fold for HIV-1 X4 (*p*-value < 0.0001) and 1.9-fold for HIV-1 R5 (*p*-value = 0.0050). The *Mtb* pathogenic strain, H37Rv, strongly blocked *trans*-infection of HIV-1 X4 and R5 virus by 5.2- and 3.4-fold respectively (*p*-value < 0.0001), and EU127 by 1.4-fold for HIV-1 X4 (*p*-value = 0.0009) and 1.5-fold for HIV-1 R5 (*p*-value < 0.0001).
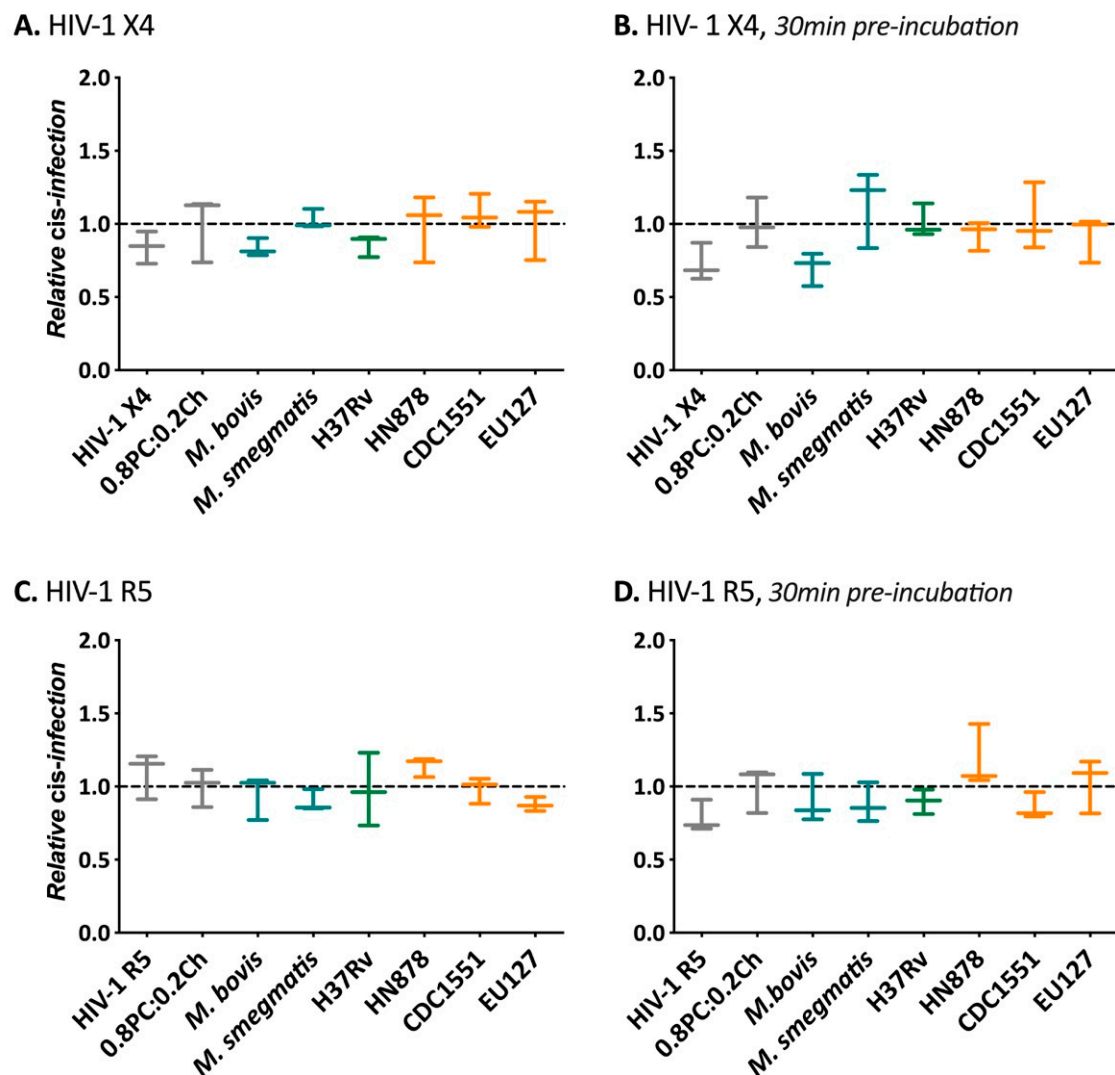
Figure 3. Influence of *Mycobacterium* liposomes on HIV-1 *cis*-infection. Cells were infected with 8 ng CA-p24 of (**A**,**B**) pSG3-LAI (HIV-1 X4), (**C**,**D**) pSG3-BAL (HIV-1 R5) and pSG3Δenv (ΔpSG3) where (**A**,**C**) virus input with 100 ng of liposomes at the same time or (**B**,**D**) 100 ng of liposomes added to TZM-bl cells 30 min prior to adding virus. 48 h after infection cells were lysed to measure luciferase activity (relative light unit, RLU). The RLUs produced for each experiment were normalised to the average value of the negative control 0.8PC:0.2Ch liposomes. 0.8PC:0.2Ch is used here as a negative control and reference. For the data shown, *n* = 3. Mann–Whitney unpaired t-test was performed for (**A**–**D**).

Conversely, only small and variable effects were observed for *M. smegmatis*, *Mtb* HN878 and CDC1551. *Mtb* HN878 increased *trans*-infection efficacy of HIV X4 by 1.2-fold (*p*-value = 0.0052), whilst there was no effect on X4 *trans*-infection by *M. smegmatis* or *Mtb* CDC1551 liposomes. Conversely, HIV-1 R5 *trans*-infection exhibited the opposite

effect, whereby HN878 liposomes did not affect capture-transfer but *M. smegmatis* and *Mtb* CDC1551 liposomes increased the efficacy of R5 by 1.3-fold (*p*-value = 0.0190) and 1.2-fold (*p*-value = 0.0414), respectively.

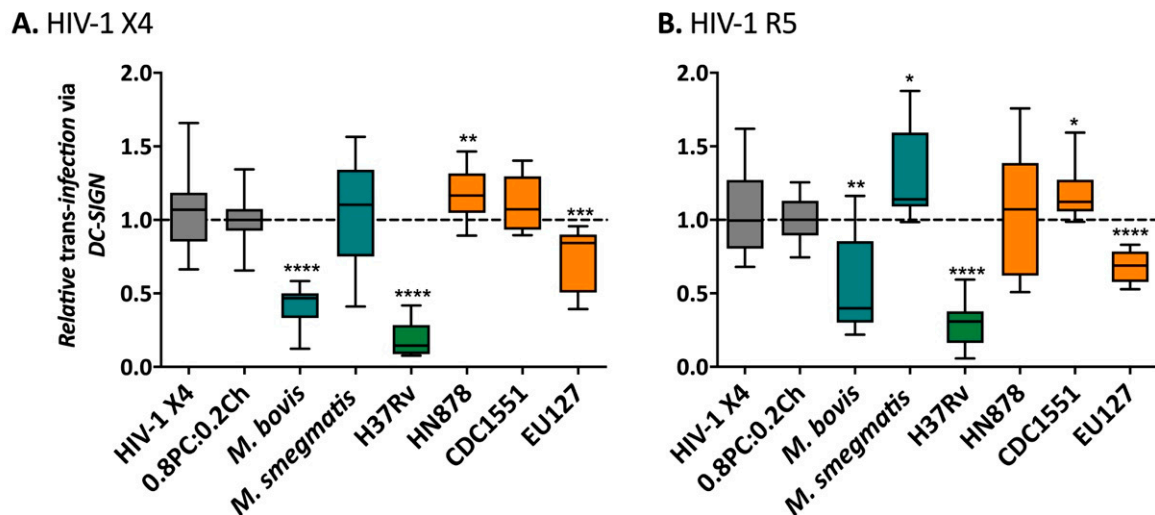**Figure 4.** Influence of the presence of *Mycobacterium* liposomes on HIV-1 *trans*-infection via Raji-DC-SIGN cells. (**A**) 12.5 ng CA-p24 pSG3-LAI (HIV-1 X4) or (**B**) 20 ng CA-p24 pSG3-BAL (HIV-1 R5). After capture the cells were washed and co-cultured with TZM-bl cells. The luciferase activity (RLU) was read after 48 h. The RLUs produced for each experiment were normalised to the average value of the negative control 0.8PC:0.2Ch liposomes. The data shown are a pool of at least two independent experiments where $n \geq 3$ in total. Mann–Whitney unpaired *t*-test was performed for (**A**,**B**) and *p*- value represented with * for *p*-value < 0.05, ** for *p*-value < 0.01, *** for *p*-value < 0.001, **** for *p*-value < 0.0001.

The impact of *M. smegmatis*, *Mtb* HN878 and CDC1551 total lipids on HIV-1 X4 and R5 *trans*-infection via DC-SIGN was minimal compared to the effect *M. bovis*, *Mtb* H37Rv and EU127, suggesting that glycolipids from these three strains could bind DC-SIGN thereby blocking virus *trans*-infection of the target cells.

2.4. Implication of SL1, PDIM and TDM Lipids in HIV-1 Trans-Infection Mediated by DC-SIGN

To further investigate the observed disruption of HIV-1 *trans*-infection by *Mtb* H37Rv glycolipids associated into liposomes, we compared the influence of total lipids from a variant H37Rv strain obtained from a different lab: H37RvMA (Figure 5) where the two lineages are differing in the number of local passage, inducing genotypic variation [74]. Raji-DC-SIGN were pre-incubated with liposomes prior to HIV-1 X4 (Figure 5A) or HIV-1 R5 (Figure 5B) capture-transfer to TZM-bl cells. Interestingly, while the presence of H37RvAE liposomes decreased HIV-1 X4 and R5 *trans*-infection via DC-SIGN to 0.35 (*p*-value = 0.0004) and 0.22 efficacy (*p*-value = 0.0004), H37RvMA did not affect virus capture-transfer with a mean efficacy of 1.09 (HIV-1 X4) and 0.98 (HIV-1 R5). Specific mutations are observed in H37RvAE compared to H37RvMA, including mutation in *ppsA* that encodes a multidomain polyketide synthase involved in PDIM biosynthesis [74]. While mouse passaged H37Rv strains do produce PDIM, it is likely that variations in PDIM levels occur in H37RvAE and H37RvMA liposomes, interfering with virus DC-SIGN receptor recognition. Given the low sensitivity of the TLC method in detecting the incorporated mycobacterial lipids (Figure 2), it is difficult to quantify this difference in PDIM levels in liposomes derived from the lipids of the two H37Rv strains.

In order to identify glycolipids from *Mtb* H37Rv that influence HIV-1 *trans*-infection via DC-SIGN, total lipids from H37Rv were fractionated and the fractions obtained were associated into liposomes to assess their impact on HIV-1 *trans*-infection (Figure 6A). For both virus tropisms, we observed inhibition of virus capture-transfer via DC-SIGN with liposomes derived from fractions 2 and 4 by 6.4 and 5-fold for HIV-1 X4 and 14.5 and

6.6-fold for HIV-1 R5, respectively. Fractions 1 and 5 liposomes also inhibited virus *trans*-infection but with a weaker effect with a decrease of 1.4-fold for HIV-1 X4 and 1.2-fold for HIV-1 R5 and an inhibition of 1.8-fold for HIV-1 X4 and 1.5-fold for HIV-R5, respectively. The influence of liposomes made with fractions 1, 3 and 7 was variable between replicates and virus tropism. TLC analyses (Figure S3) revealed the presence of PDIM and SL in fraction 2 and TDM in fractions 4 to 7 where TDM concentration decreased through fractionation. These results suggest that PDIM, SL and TDM are involved in disruption of DC-SIGN mediated HIV-1 *trans*-infection.
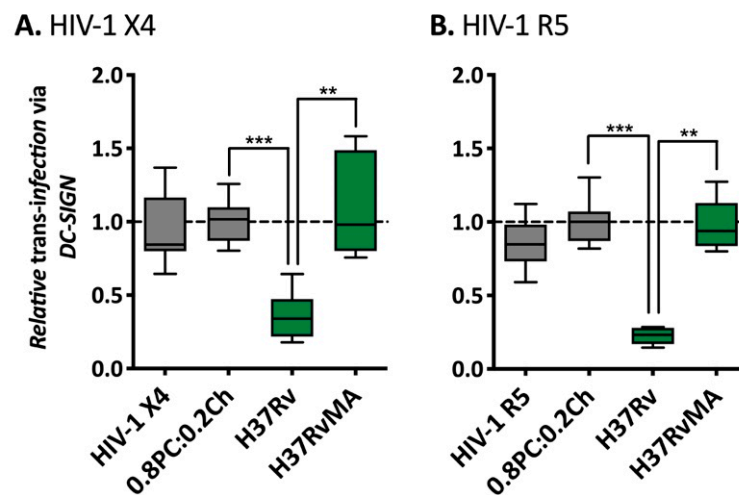

Figure 5. Comparison of the influence different H37Rv on HIV-1 *trans*-infection via Raji-DC-SIGN cells. (**A**) 12.5 ng CA-p24 pSG3-LAI (HIV-1 X4) or (**B**) 20 ng CA-p24 pSG3-BAL (HIV-1 R5). After capture the cells were washed and co-cultured with TZM-bl cells. The luciferase activity was read after 48 h. The RLUs produced for each experiment were normalised to the average value of the negative control 0.8PC:0.2Ch liposomes. The data shown are a pool of at least two independent experiments where $n \geq 6$ in total. Mann–Whitney unpaired t-test was performed for (**A**,**B**) and *p*-value represented with * for *p*-value < 0.05, ** for *p*-value < 0.01, *** for *p*-value < 0.001, **** for *p*-value < 0.0001.

The role of SL1 was further investigated by generating liposomes from total lipids isolated from an H37Rv papA1Δ mutant (mutant missing the polyketide associated-protein-1, papA1, involved in biogenesis of SL1 and resulting in the absence of SL1 production) in parallel to liposomes with H37Rv papA1Δ total lipids complemented with soluble SL1 (Figure 6B). When we studied the impact of these liposomes on HIV-1 X4 (1) and HIV-1 R5 (2) *trans*-infection mediated by DC-SIGN, we observed that papA1Δ liposomes only decreased virus capture-transfer by 1.1-fold for HIV-1 X4 (*p*-value = 0.0053) and 1.2-fold for HIV-1 R5 (*p*-value = 0.0030) while H37Rv blocked *trans*-infection via DC-SIGN by 3.2-fold (*p*-value < 0.0001) for HIV-1 X4 and 3.1-fold (*p*-value < 0.0001) for HIV-1 R5. Interestingly, liposomes composed of papA1Δ total lipids complemented with SL1 were shown to cause strong inhibition of 3.4-fold for HIV-1 X4 (*p*-value < 0.0001) and 4.1-fold for HIV-1 R5 (*p*-value< 0.0001) *trans*-infection, indicating that SL1 expressed on H37Rv binds the DC-SIGN receptor, blocking HIV-1 *trans*-infection via this C-type lectin.
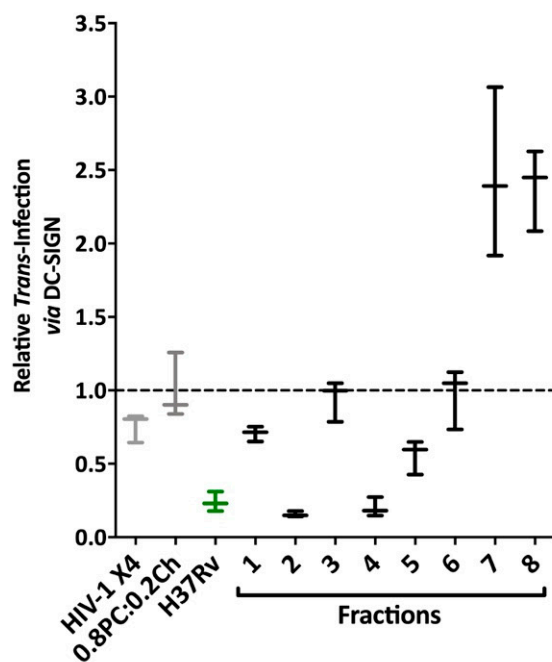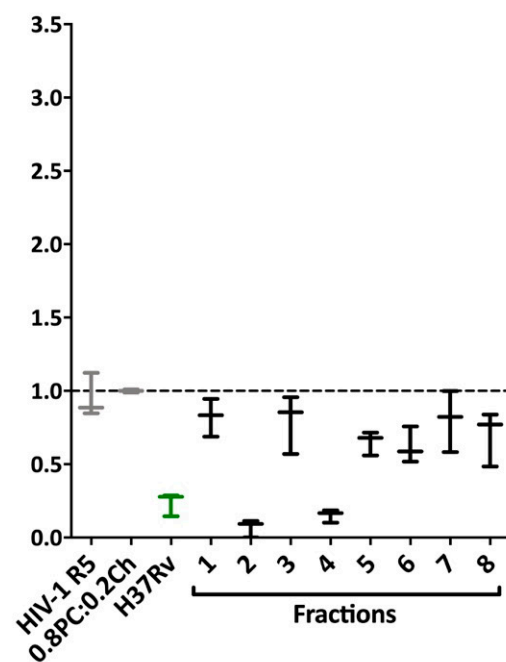
A. Impact of H37Rv lipids Fractions on HIV-1 *trans*-infection *via* Raji-DC-SIGN

(1) HIV-1 X4

(2) HIV-1 R5

B. Role of SL1 in HIV-1 *trans*-infection *via* Raji-DC-SIGN

(1) HIV-1 X4
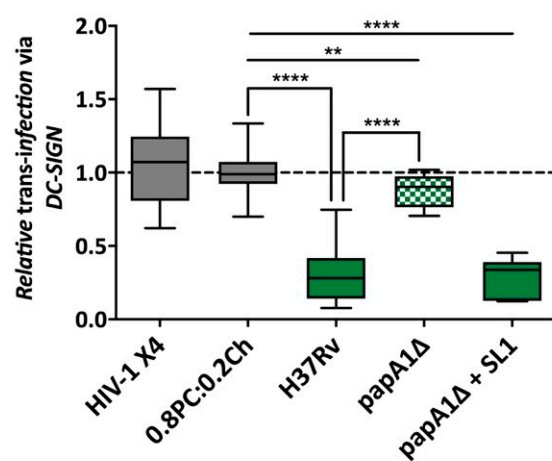
(2) HIV-1 R5
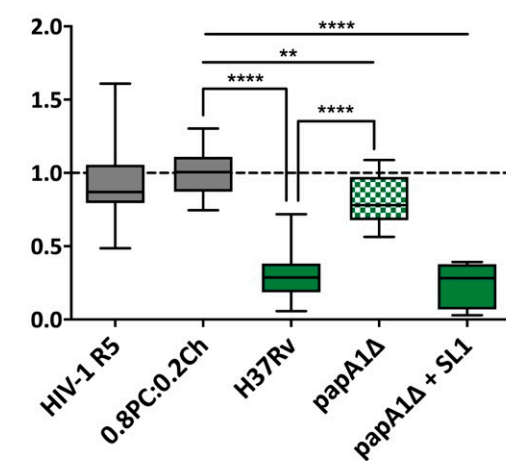
Figure 6. Role of H37Rv glycolipids in HIV-1 *trans*-infection via DC-SIGN. (**A**) H37Rv fractions 1 to 8 have been integrated into liposomes following the ratio 0.6PC:0.2Ch:0.2fraction and were tested on HIV-1 *trans*-infection via DC-SIGN in parallel of 0.8PC:0.2Ch and H37Rv liposomes. The data shown are from one experiment, $n = 3$. (**B**) H37Rv papA1Δ and H37Rv papA1Δ + SL1 were tested in parallel of 0.8PC:0.2Ch and H37Rv liposomes on HIV-1 *trans*-infection. The data shown are a pool of at least two independent experiments where $n \geq 6$ in total. For (**A,B**) 0.5×10^6 Raji DC-SIGN were pre-incubated during 30 min with 100 μg liposomes or 50 μL of media. The cells were then incubated for 2 h with HIV-1 pseudo-typed virus (1) 12.5 ng CA-p24 pSG3-LAI (HIV-1 X4) or (2) 20 ng CA-p24 pSG3-BAL (HIV-1 R5). After capture the cells were washed and co-cultured with TZM-bl cells. The luciferase activity was read after 48 h. The RLUs produced for each experiment were normalised to the average value of the negative control 0.8PC:0.2Ch liposomes. Mann–Whitney unpaired t-test was performed for (**A,B**) and *p*-value represented with * for *p*-value < 0.05, ** for *p*-value < 0.01, *** for *p*-value < 0.001, **** for *p*-value < 0.0001.

2.5. Differential Effects of Mtb Glycolipids on HIV-1 Trans-Infection Mediated via iDC and mDC

We next studied the impact of *Mycobacterium* liposomes on *trans*-infection of HIV-1 via DCs, the physiological relevant cell-types mediating HIV-1 capture-transfer. DCs were pre-incubated with liposomes before capture and transfer of HIV-1 X4 or R5 by DCs at different stages of maturation: iDCs (Figure 7A,B) and mDCs (Figure 7C,D). Interestingly, as observed with the Raji-DC-SIGN in vitro assays, HIV-1 X4 and R5 iDC mediated *trans*-infections were inhibited by 1.4- and 1.5-fold (*p*-value = 0.0450) in the presence of *M. bovis*; by 1.8- (*p*-value = 0.0025) and 2.1-fold (*p*-value = 0.0002) in the presence of H37Rv; and by 1.7- (*p*-value = 0.0011) and 1.6-fold (*p*-value = 0.0034) in the presence of EU127 liposomes, respectively. On the contrary, *M. smegmatis*, as well as *Mtb* HN878 and CDC1551 liposomes showed a trend toward increasing HIV-1 *trans*-infection via iDCs by 1.6-fold (HIV-1 R5); 1.3- (HIV-1 X4) and 1.5-fold (HIV-1 R5); and by 1.4- (HIV-1 X4) and 1.6-fold (HIV-1 R5, *p*-value = 0.0220) respectively (Figure 7A,B). These observations suggest that *M. bovis*, *Mtb* H37Rv and EU127 glycolipids are recognised by the DC-SIGN receptor expressed on iDCs causing inhibition of HIV-1 capture and transfer to target cells.

In parallel, iDCs were grown in the presence of poly(I:C) to allow maturation into mDCs and further used to mediate HIV-1 *trans*-infection to TZM-bl in the presence of *Mycobacterium* liposomes (Figure 7C,D). Although we observed variant efficiency of virus capture and transfer reflecting donor-to-donor variation, trends were observed when comparing the different mycobacterial strains. The presence of *M. bovis* liposomes prior to HIV-1 X4 and R5 capture-transfer via mDCs significantly inhibited the efficiency of *trans*-infection by 1.3- (*p*-value = 0.0071) and 1.5-fold (*p*-value = 0.0047) respectively. Similarly, H37Rv and CDC1551 liposomes blocked HIV-1 R5 viruses by 1.3- (*p*-value = 0.0052) and 1.6-fold (*p*-value = 0.0009) compared to the negative control 0.8PC:0.2Ch. For HN878, one mDCs donor did exhibit heightened transfer of HIV-1 X4 by 2.5-fold and which seemed to follow a trend of activation. Interestingly, cells from another donor showed an increase of HIV-1 X4 *trans*-infection in the presence of *M. smegmatis*. There is a clear variation in the impact of *Mycobacterium* liposomes on HIV-1 X4 and R5 *trans*-infection, depending on the stage of DC maturation and virus tropism. These results suggest that the DC-SIGN receptor is likely involved in HIV-1 DCs mediated *trans*-infection as well as other receptors expressed by iDCs and mDCs, explaining variations between the cells types used.

The above is supported when analyzing the effect of mannan, a DC-SIGN receptor antagonist, on HIV-1 *trans*-infection mediated by Raji-DC-SIGN, iDCs or mDCs (Figure S4). We tested two different concentrations of mannan, which was pre-incubated with each cell type prior to HIV-1 X4 *trans*-infection, as was performed for liposomes. We observed that Raji-DC-SIGN HIV-1 X4 *trans*-infection of TZM-bl cells is strongly inhibited with both concentrations of mannan tested with efficacy decreased to 0.16 with 20 µg/mL and in total with 2 mg/mL of mannan compared to virus alone. Blocking the DC-SIGN receptor with mannan on iDCs seems to not fully inhibit HIV-1 *trans*-infection. Indeed capture-transfer was partially blocked and displayed a dose dependent effect: 20 µg/mL mannan reduced efficacy by 1.5-fold and 2 mg/mL by 2.0-fold. Concerning capture-transfer via mDCs, we did not observe any inhibition to HIV-1 X4 capture-transfer but an increase was observed with 2 mg/mL by 1.6-fold. DC-SIGN recognition from antagonists such as mannan can decrease HIV-1 *trans*-infection via iDCs whereas on mDCs, the DC-SIGN antagonist could be seen to increase HIV-1 *trans*-infection at the highest concentration.
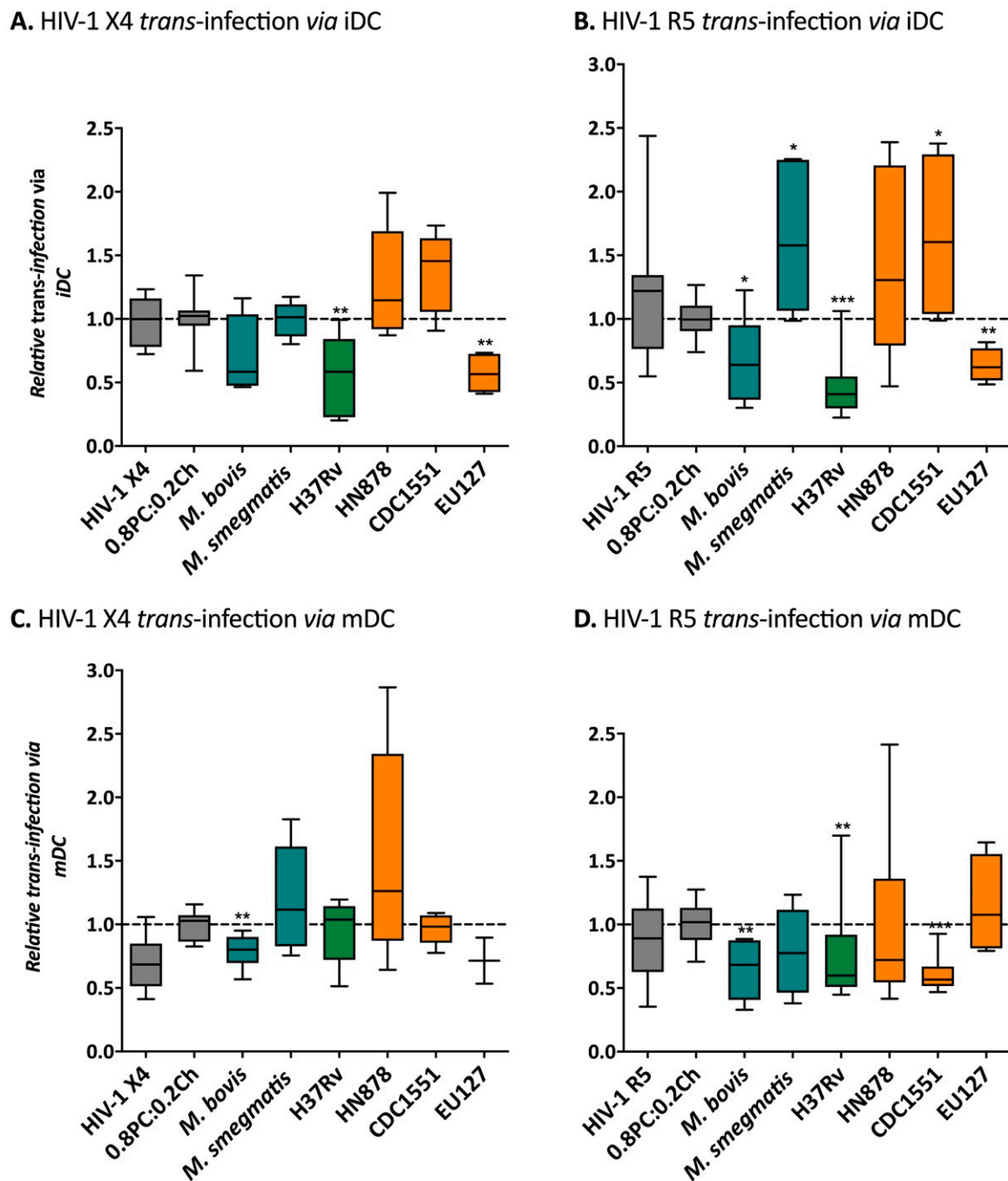
Figure 7. Influence of *Mycobacterium* liposomes on HIV-1 *trans*-infection via iDCs or mDCs. (**A**) and (**B**) iDCS, (**C,D**) mDCs, was pre-incubation for 30 min with 100 µg of liposomes or 50 µL of media. The cells were then incubated 2h with HIV-1 pseudo-typed virus: 12.5 ng CA-p24 pSG3-LAI (HIV-1 X4, panels (**A,C**)) or 20 ng CA-p24 pSG3-BAL (HIV-1 R5, panels (**B,D**)). For the data shown, the experiment has been performed using cells isolated from on at least two different donors where $n \geq 3$ in total. The RLUs produced for each experiment were normalised to the average value of the negative control 0.8PC:0.2Ch liposomes. Mann–Whitney unpaired t-test was performed for (**A–D**) and *p*-value represented with * for *p*-value < 0.05, ** for *p*-value < 0.01, *** for *p*-value < 0.001, **** for *p*-value < 0.0001.

3. Discussion

Here we investigated the role of *Mycobacterium* lipid extracts presented via liposomes on influencing HIV-1 *cis*- and *trans*-infection. From this preliminary analysis of utilising generated liposomes containing lipid extract antigen from variant pathogenic (e.g., Mtb H37Rv, HN878, CDC1551 and EU127) and non-pathogenic (*M. bovis* and *M. smegmatis*)

Mycobacterium strains we observed no difference between strains for influencing HIV-1 X4 or HIV-1 R5 direct infection of TZM-bl cells. The bacterial glycolipid antigens presented on liposomes therefore did not interfere with direct HIV-1 entry to target cells via either the CCR5 or CXCR4 co-receptor. This indicates that the interaction and binding of HIV-1 envelope protein sub-unit gp120 with CD4 receptor and co-receptors CCR5 and CXCR4 is not impacted by mycobacterial glycolipids. These results support that the mechanisms involved in enhancement of HIV-1 replication observed in co-infected patient [75,76] is most likely due to the modulation of the immune system by *Mtb* infection and do not involve an increase of HIV-1 entry efficacy via direct interaction with *Mtb* components.

However, our data suggest that *Mtb* glycolipids potentially impair or enhance HIV-1 *trans*-infection, where DCs capture and present virus to CD4 T cells, with important implications for virus transmission and dissemination. The capture of infectious virions and subsequent transmission to uninfected cells occurs by attachment of the glycoprotein Env to DC receptors such as MR or DC-SIGN [8–10,13,77,78]. We demonstrate that *trans*-infection of both R5 and X4 tropic HIV-1, mediated by DC-SIGN receptor, was impaired in the presence of *Mtb* glycolipids from *M. bovis*, *Mtb* H37Rv and *Mtb* EU127 strains. Unexpectedly, we identified TDM, SL1 and PDIM glycolipids to be involved in DC-SIGN recognition and impairment of HIV-1 *trans*-infection by using *Mtb* H37Rv total lipids fractionation. TDM is a major contributor of the immune simulation and is known to interact with C-type lectin receptor Mincle expressed on macrophages [37,79] but not DC-SIGN. Conversely, *Mtb* glycolipids PIMs, LM and LAM, identified to interact with C-type lectin receptors due to their mannoside caps [49–51], present in fraction 8 on H37Rv total lipids fractionation in our assays, did not show a clear impact on HIV-1 *trans*-infection mediated by DC-SIGN receptor. Concerning SL1, its role in *Mycobacterium* pathogenicity remains unclear [80,81]. In our model, we demonstrated using total lipids extract from the H37Rv mutant papA1Δ associated into liposomes, that SL1 is critical in the inhibition of DC-SIGN mediated HIV-1 *trans*-infection from *Mtb* H37Rv, suggesting SL1 interactions with DC-SIGN receptor. Additionally, the comparison between H37RvMA strains and H37RvAE differing from their origin and PDIM biosynthesis and composition [74], reveals the implication of PDIM in DC-SIGN/SL1 interactions. Indeed, the impairment of HIV-1 DC-SIGN mediated *trans*-infection with glycolipids from H37RvAE is lost using liposomes with total lipids extracted from H37RvMA. PDIM is known to be able to mask PAMPs to escape from macrophage recognition [45,46,48], suggesting that in our system, high levels of expression of PDIM in H37RvMA could mask SL1 interactions with DC-SIGN and not interfere with virus capture. Nevertheless, the interaction of PDIM, SL1 and TDM with DC-SIGN receptors remains to be characterised.

We tested the impact of the *Mtb* glycolipids associated into liposomes on HIV-1 *trans*-infection mediated by DCs at different stage of maturation. Our findings indicate that *M. bovis*, *Mtb* H37Rv and *Mtb* EU127 are able to inhibit HIV-1 *trans*-infection via iDCs. The similar observations obtained on HIV-1 capture/transfer mediated by DC-SIGN, suggests the involvement of DC-SIGN receptors in the inhibition of virus capture by iDC in the presence of glycolipids from these strains. Conversely, *M. smegmatis*, *Mtb* HN878 and *Mtb* CDC1551 liposomes showed a trend toward increasing HIV-1 *trans*-infection via iDCs. These results suggest the involvement of receptors other than DC-SIGN, such as MR, in *Mtb* antigen recognition, impacting HIV-1 *trans*-infection via mDC [10,11]. Moreover, the stage of DCs maturation influences HIV-1 *trans*-infection, where mDCs are more efficient at supporting virus *trans*-infection using different mechanisms compared to iDCs [19,82–84], glycolipids from *M. smegmatis*, *Mtb* HN878 and CDC1551 could activate iDCs maturation by pattern recognition receptors (PRRs) recognition and improve HIV-1 *trans*-infection efficacy. Interestingly, the impact of *Mtb* liposomes on mDCs mediated HIV-1 *trans*-infection varies from the experiments using iDCs. The variations observed between cell types supports the hypothesis that receptors other than DC-SIGN can impact HIV-1 capture and transfer and which can be differentially modulated by *Mtb* glycolipids. These complex interactions between bacterial antigens and immune cells will undoubtedly influence the

ensuing immune responses generated. HIV-1 *trans*-infection mediated by mDCs, involved the receptor Siglec [16–20,84]. The influence reported here of *Mtb* liposomes on HIV-1 *trans*-infection mediated may be due to interactions with other PRRs, influencing Siglec expression, or direct interaction with Siglec.

Collectively, our findings indicate that variant strains of *Mtb* can provide differential effects on HIV-1 *trans*-infection which has the potential to influence HIV-1 disease course in co-infected individuals. Studying HIV-1 *trans*-infection mediated via DC-SIGN receptor represents a valuable alternative in vitro model to analyse DC-SIGN interactions with bacterial glycolipid components. Additionally, liposomes technology represents a useful technique to best mimic lipid distribution and antigen presentation on the mycobacterial cell wall. The activation of PRR signaling pathways by *Mtb* PAMPs leads to the activation of HIV-1 replication and infection [85] through various mechanisms including the modification/translocation of transcription factors [86,87], activation of NF-κB pathways, or cytokine production [88–91]. Liposome technology will provide a means to study the effects that *Mtb* antigens can exert on cell signaling and induction of immune responses impacting HIV-1 infection, and more generally, the effect of bacterial antigens on the immune responses.

4. Materials and Methods

4.1. Commercial Lipids

Cholesterol (Ch) and phosphatidylcholine (PC) were purchased from Sigma-Aldrich (Sigma-Aldrich, St. Louis, MO, USA), and SL1 lipid solutions from BEI Resources.

4.2. M. Tuberculosis Strains and H37Rv Mutants

Mtb H37RvAE was used for all experiments unless otherwise mentioned. The EU127 *Mtb* strain was selected from a biobank of *Mtb* strains collected in a clinical study conducted at the uBuntu clinic in Site B, Khayelitsha, a peri-urban township 30 km outside of Cape Town, South Africa. Spoligotyping of this indicated that EU127 was a Beijing genotype. The HN878, CDC1551 and H37RvMA *Mtb* isolates were propagated as part of the same strain library and included as controls. H37RvAE Δ papA1 was constructed by specialized transduction as described [92].

Mtb glycerol stocks were inoculated into 10 mL of 7H9 (BD, Franklin Lakes, NJ, USA) media with ADC (BD, Franklin Lakes, NJ, USA) and 0.05% Tween 80 (Sigma-Aldrich, St. Louis, MO, USA) supplementation and cultured at 37° for 10 days, with gentle agitation every two days. On day 10, 1 mL of this culture was used to inoculate 100 mL of 7H9 media with ADC supplementation (without Tween 80) and cultured for a further 10 days at 37 °C without shaking. Cultures were centrifuged at 8000× rpm for 10 min to pellet the cells. The supernatant was removed and discarded, and the pellet was resuspended in 1 mL of PBS. *Mtb* was killed by boiling cell suspensions at 80 °C for 1 h and used from lipid extractions and preparation of liposomes.

4.3. Lipids Extractions

Total lipid extracts were obtained from culture pellet of *M. bovis* (BCG), *M. smegmatis* (MC²155), *Mtb* H37Rv (H37RvAE), H37RvMA, H37RvAE Δ papA1, HN878, CDC1551 and EU127 following standard procedures as described [93]. Shortly, a solution of $CHCl_3$:MeOH:H_2O was added to the bacterial pellet and kept at 50 °C for 3h. After centrifugation at 3000× *g* rpm, a mix of $CHCl_3$:H_2O was added to the supernatant and centrifuged after mixing. The bottom phase obtained was then washed 2× *g* by with a mix of $CHCl_3$:MeOH:H_2O (3:47:48 proportions) and heat at 55 °C to obtained a dry pellet.

For H37Rv (H37RvAE) lipids fractionation, 2 mg of total lipid extract from *Mtb* H37RvAE was fractioned using a silica column. The column was pre-washed with chloroform (3× void volume) before the sample was added. Once the input sample was added onto the column, 100 mL of chloroform was added to start flow through collection. A mix of $CHCl_3$:MeOH solvent was passed through the column with a progressive increase

in the proportion of methanol (99:1, 1–8 collection tubes; 98:2, 9–15 collection tubes; 97:3, 16–23 collection tubes; 95:5, 24–31 collection tubes; 93:7, 32–49 collection tubes; 90:10, 50–57 collection tubes and 80:20, 58–63 collection tubes). For the analyses of H37RvAE, collection tubes 1 to 9 were pooled as Fraction 1; 10 to 13 pooled as Fraction 2; 14 to 18 pooled as Fraction 3; 19 to 27 pooled as Fraction 4; 28 to 32 pooled as Fraction 5; 33 to 36 pooled as Fraction 6, 37 to 44 pooled as Fraction 7 and 45 to 63 pooled as Fraction 8.

4.4. Liposomes

All dried lipid pellets were solubilised in $CHCl_3$:MeOH (2:1 proportion) and PC and Ch were solubilised in chloroform. Liposomes were generated with a mix of PC and Ch in 0.8PC:0.2Ch proportion for liposomes without *Mycobacterium* lipids; a mix of PC, Ch and total lipids extracted from BCG, MC^2155, H37RvAE, H37RvMA, H37Rv papA1Δ, H37RvAE Fractions, HN878, CDC1551 and EU127 in 0.6PC:0.2Ch:0.2 *Mycobacterium* proportion; a mix of PC, Ch, H37Rv papA1Δ and SL1 lipids in 0.6PC:0.2Ch:1.9:0.1SL1; or a mix of PC, Ch and PDIM lipids in 7.8PC:0.2Ch:0.2PDIM proportion. After the different lipids were mixed together in chloroform solution (2 mg in total), the chloroform was then evaporated with nitrogen gas for 30 min forming a film of dried lipids. Liposomes were hydrated by addition of Roswell Park Memorial Institute (RPMI-1640, Thermo Fisher Scientific, Waltham, MA, USA), Dulbecco Modified Eagle Medium (DMEM, Thermo Fisher Scientific, Waltham, MA, USA), Phosphate-Buffered Saline (PBS, Thermo Fisher Scientific, Waltham, MA, USA), or sterile water. Liposomes were then incubated at 55 °C for 30 min with vortexing (final concentration 10 mg/mL). The preparations were subsequently sonicated for 30 min at 4 °C.

For NanoSight analyses of liposomes, 0.8PC:0.2Ch liposomes were filtered using the Avanti® Mini-Extruder system after sonication. Liposome solutions were filtered through a 100 or 200 nm polycarbonate filter under 50 °C temperature to produce 100 and 200 nm 0.8PC:0.2Ch liposome diameters.

4.5. Liposomes Characterisation

For TLC analyses, 10 μL of 0.8PC:0.2Ch, BCG and H37RvAE liposomes made in sterile water, SL, TDM, PIMs, PDIM lipid solution or H37RvAE lipid Fractions 1 to 8 were spotted and dried on a silica gel 60 F254 plate (Sigma-Aldrich, St. Louis, MO, USA). Sample separation occurred in 60:16:2 $CHCl_3$:MeOH:H_2O solvent and was visualised by staining with molybdophosphoric acid (MPA) and charring.

Visualisation, particle concentration and the size distribution of the generated liposomes were evaluated using the NanoSight NS300 instrument (Malvern Panatical, Malvern, UK) and using Nanoparticle Tracking Analysis (NTA) software. Videos were recording at camera level 13. The post-acquisition settings were with a minimum detection threshold 7, automatic blur and automatic minimum expected particle size. 0.8PC:0.2Ch, BCG and H37RvAE liposome made in PBS were diluted 1:1000–1:2000 in PBS for each sample and three 60 s videos were recorded and analysed.

4.6. Cells

293T and TZM-bl (NIH AIDS) cells were maintained at 37 °C 5% CO_2 in DMEM supplemented with 10% FBS, L-glutamine, 100 U/mL penicillin and 100 mg/mL streptomycin. Raji-DC-SIGN (NIH AIDS) were cultured at 37 °C 5% CO_2 in RPMI-1640 containing L-glutamine, supplemented with 10% FBS, 100 U/mL penicillin and 100 mg/mL streptomycin.

Human blood monocytes were isolated in buffy coats from healthy donors by using Ficoll gradient and a subsequent CD14 selection step using the MACS system (Miltenyi Biotec, Bergisch Gladbach, Germany). Purified monocytes were cultured RPMI-1640 containing L-glutamine supplemented with 10% FBS serum 100 U/mL penicillin, 100 mg/mL streptomycin, 70 ng/mL human IL-4 (Thermo Fisher Scientific, Waltham, MA, USA) and 50 ng/mL human GM-CSF (Thermo Fisher Scientific, Waltham, MA, USA) for differentia-

tion into immature dendritic cells (iDC). The iDCs were harvested after 6 days of incubation. Mature monocyte derived dendritic cells (mDCs) were isolated from fresh iDCs. At day 620 µg/mL of Poly(I:C) (Sigma-Aldrich, St. Louis, MO, USA) was added to iDCs media. The mDCs cells were harvested after 18–24 h of incubation at 37 °C, 5% CO_2.

4.7. Cell Viability in the Presence of Liposomes

3×10^4 TZM-bl cells in 250 µL media per well were seeded in 96-well plates. After 24 h at 37 °C 5% CO_2, the cells were incubated with 1000, 100, 10 and 1 ng of 0.8PC:0.2Ch liposomes in 250 µL total volume. After 48 h incubation at 37 °C 5% CO_2 the media was removed and the cells harvested via trypsin treatment and fixed in 2% PFA (Sigma-Aldrich, St. Louis, MO, USA). After fixation, the cells were re-suspended in PBS and the viability was analysed by standard flow cytometry measuring forward and side scatter to determine live from dead cell populations. BD Accuri™ C6 was used to record 10,000 events for each sample and data analysis was performed using the BD Accuri™ C6 Plus software. Furthermore, no differences in cell recoveries were observed following culturing in the presence of the variant concentrations of liposomes.

4.8. Virus Production

One day prior to transfection 1.2×10^6 293T cells were seeded in a 10 cm dish in 8 mL of media. After 24 h, the cells were transfected using the Lipofectamine standard method where 2 µg of HIV-1 envelope plasmid BAL (R5 tropism, NIH AIDS) or LAI (X4 tropism, NIH AIDS), and 2 µg of the backbone pSG3Δ*env* plasmid (NIH AIDS) were mixed in 300 µL of OptiMEM (Thermo Fisher Scientific, Waltham, MA, USA). Separately, 24 µL of Lipofectamine was mixed with 276 µL of OptiMEM and 300 µL of this was added to the DNA mix. After 30 min incubation at RT, the Lipofectamine/DNA mixture was added dropwise to 293T cells with 1 mL of OptiMEM. After 6h, the media was replaced with fresh DMEM and the pseudo-typed virus stock (supernatant) was harvested after further 48 h of incubation at 37 °C 5% CO_2. Viruses were stored at −80 °C and virus concentrations were quantified by measuring CA-p24 antigen levels by ELISA (Aalto Bio Reagents, Dublin, Ireland).

4.9. HIV-1 Cis-Infection

One day prior to infection, 3×10^4 TZM-bl cells in 250 µL of media per well were seeded in 96-well plates. In scenario one, liposomes suspension in DMEM was added to the cells at the same time virus was added. 8ng CA-p24 of pSG3-LAI, pSG3-BAL pseudo-typed virus was mixed with 100 ng liposomes in 50 µL total volume and added to the TZM-bl cells. After 2 h incubation at 37 °C 5% CO_2, 200 µL of media was added and the infection measured after 48 h. In the second scenario, liposome suspensions in DMEM were added to the cells prior to virus input. 50 µL of 100ng of liposome was added to the TZM-bl cells. After 30 min incubation at 37 °C and 5% CO_2, 8 ng CA-p24 of pSG3-LAI or pSG3-BAL pseudo-typed virus was added and incubated for 2 h as described above. Following this incubation, 200 µL of media was added to each well and incubated for 48 h. For both scenarios, after 48 h of infection the cells were washed with PBS, and 20 µL of lysis Buffer (Promega, Madison, WI, USA) was added per well. Luciferase activity was determined using the Luciferase Assay kit (Promega, Madison, WI, USA) and FLUOStar Omega luminometer (BMG LabTech, Ortenberg, Germany) following the manufacturer's instructions. Infections with pSG3Δenv virus were used as negative control.

4.10. HIV-1 Trans-Infection

One day prior to capture/transfer, 3×10^4 TZM-bl cells per well were seeded on 96-well plates and cultured overnight. Prior virus capture, 0.5×10^6 Raji DC-SIGN, iDCs or mDCs cells were pelleted and mixed with 100 µg of liposomes in RPMI-1640 suspension. After 30 min incubation at 37 °C 5% CO_2, 12.5 ng CA-p24 pSG3Δenv, 12.5 ng CA-p24 pSG3-LAI or 25 ng CA-p24 of pSG3-BAL were added to cells for 2 h at 37 °C 5% CO_2. The cells were

then washed 4× with cold PBS and re-suspended in 45 μL of DMEM containing 30 ng/mL of Dextran. Finally, 15 μL of the suspension was used per well to infect TZM-bl cells. After 48 h at 37 °C 5% CO_2, the TZM-bl cells were lysed and luciferase activity measured as described above. Infection with pSG3Δenv virus were used as negative control.

4.11. Statistical Analysis

For all results, unpaired sample comparisons were performed using the non-parametric rank test Mann–Whitney and depict in Figures using the following: * for *p*-value < 0.05, ** for *p*-value < 0.01, *** for *p*-value < 0.001, **** for *p*-value < 0.0001. Data are represented in boxplot where the box extends from the 25th and 75th percentiles, the median is plotted at the line in the middle of the box, the whiskers represent the minimum and maximum value. All statistical analyses were performed with the Prism software.

Abbreviations

AG	Arabinogalactan
BCG	Bacille Calmette Guerin
CCR5	CC chemokine receptor 5
Ch	Cholesterol
CXCR4	CXC chemokine receptor 4
DC	Dendritic cell
DC-SIGN	Dendritic cell-specific ICAM-3-grabbing non-integrin
HIV-1	Human Immunodeficiency Virus type 1
iDC	Immature dendritic cell
LAM	lipoarabinomannan
LM	lipomannan
LTR	Long Terminal Repeat
MA	Mycolic acids
Mincle	macrophage-inducible C-type lectin
mDC	Mature dendritic cell
MR	Mannose receptor
Mtb	*Mycobacterium tuberculosis*
PAMPs	Pathogen associated molecular patterns

papA1	Polyketide associated-protein-1
PC	Phosphatidylcholine
PDIM	Phthiocerol dimycocerosate
PG	Peptidoglycan
PGL	Phenolic glycolipids
PIM	Phosphatidylinositol mannoside
PRR	Pattern recognition receptors
SL	Sulfolipid
TB	Tuberculosis
TDM	Trehalose dimycolate
TLC	Thin-layer chromatography

References

1. *World Health Organization Global Tuberculosis Report*; WHO: Geneva, Switzerland, 2020.
2. Sullivan, Z.A.; Wong, E.B.; Ndung'u, T.; Kasprowicz, V.O.; Bishai, W.R. Latent and Active Tuberculosis Infection Increase Immune Activation in Individuals Co-Infected with HIV. *EBioMedicine* **2015**, *2*, 334–340. [CrossRef]
3. Bell, L.C.K.; Noursadeghi, M. Pathogenesis of HIV-1 and *Mycobacterium tuberculosis* co-infection. *Nat. Rev. Microbiol.* **2018**, *16*, 80–90. [CrossRef] [PubMed]
4. Waters, R.; Ndengane, M.; Abrahams, M.-R.; Diedrich, C.R.; Wilkinson, R.J.; Coussens, A.K. The Mtb-HIV syndemic interaction: Why treating *M. tuberculosis* infection may be crucial for HIV-1 eradication. *Future Virol.* **2020**, *15*, 101–125. [CrossRef]
5. Naqvi, K.F.; Endsley, J.J. Myeloid C-Type Lectin Receptors in Tuberculosis and HIV Immunity: Insights Into Co-infection? *Front. Cell. Infect. Microbiol.* **2020**, *10*, 263. [CrossRef]
6. Nguyen, D.G.; Hildreth, J.E.K. Involvement of macrophage mannose receptor in the binding and transmission of HIV by macrophages. *Eur. J. Immunol.* **2003**, *33*, 483–493. [CrossRef] [PubMed]
7. Cameron, P.U.; Freudenthal, P.S.; Barker, J.M.; Gezelter, S.; Inaba, K.; Steinman, R.M. Dendritic cells exposed to human immunodeficiency virus type-1 transmit a vigorous cytopathic infection to CD4+ T cells. *Science* **1992**, *257*, 383–387. [CrossRef] [PubMed]
8. Gummuluru, S.; KewalRamani, V.N.; Emerman, M. Dendritic cell-mediated viral transfer to T cells is required for human immunodeficiency virus type 1 persistence in the face of rapid cell turnover. *J. Virol.* **2002**, *76*, 10692–10701. [CrossRef]
9. Garcia, E.; Pion, M.; Pelchen-Matthews, A.; Collinson, L.; Arrighi, J.F.; Blot, G.; Leuba, F.; Escola, J.M.; Demaurex, N.; Marsh, M.; et al. HIV-1 trafficking to the dendritic cell-T-cell infectious synapse uses a pathway of tetraspanin sorting to the immunological synapse. *Traffic* **2005**, *6*, 488–501. [CrossRef] [PubMed]
10. Sallusto, F.; Cella, M.; Danieli, C.; Lanzavecchia, A. Dendritic cells use macropinocytosis and the mannose receptor to concentrate macromolecules in the major histocompatibility complex class II compartment: Downregulation by cytokines and bacterial products. *J. Exp. Med.* **1995**, *182*, 389–400. [CrossRef]
11. Turville, S.G.; Cameron, P.U.; Handley, A.; Lin, G.; Pöhlmann, S.; Doms, R.W.; Cunningham, A.L. Diversity of receptors binding HIV on dendritic cell subsets. *Nat. Immunol.* **2002**, *3*, 975–983. [CrossRef]
12. Geijtenbeek, T.B.; Kwon, D.S.; Torensma, R.; van Vliet, S.J.; van Duijnhoven, G.C.; Middel, J.; Cornelissen, I.L.M.H.; Nottet, H.S.L.; KewalRamani, V.N.; Littman, D.R.; et al. DC-SIGN, a dendritic cell-specific HIV-1-binding protein that enhances trans-infection of T cells. *Cell* **2000**, *100*, 587–597. [CrossRef]
13. Turville, S.; Wilkinson, J.; Cameron, P.; Dable, J.; Cunningham, A.L. The role of dendritic cell C-type lectin receptors in HIV pathogenesis. *J. Leukoc. Biol.* **2003**, *74*, 710–718. [CrossRef] [PubMed]
14. Moris, A.; Pajot, A.; Blanchet, F.; Guivel-Benhassine, F.; Salcedo, M.; Schwartz, O. Dendritic cells and HIV-specific CD4+ T cells: HIV antigen presentation, T-cell activation, and viral transfer. *Blood* **2006**, *108*, 1643–1651. [CrossRef]
15. Van Montfort, T.; Nabatov, A.A.; Geijtenbeek, T.B.H.; Pollakis, G.; Paxton, W.A. Efficient capture of antibody neutralized HIV-1 by cells expressing DC-SIGN and transfer to CD4+ T lymphocytes. *J. Immunol.* **2007**, *178*, 3177–3185. [CrossRef] [PubMed]
16. Bobardt, M.D.; Saphire, A.C.S.; Hung, H.-C.; Yu, X.; Van der Schueren, B.; Zhang, Z.; David, G.; Gallay, P.A. Syndecan captures, protects, and transmits HIV to T lymphocytes. *Immunity* **2003**, *18*, 27–39. [CrossRef]
17. De Witte, L.; Bobardt, M.; Chatterji, U.; Degeest, G.; David, G.; Geijtenbeek, T.B.H.; Gallay, P. Syndecan-3 is a dendritic cell-specific attachment receptor for HIV-1. *Proc. Natl. Acad. Sci. USA* **2007**, *104*, 19464–19469. [CrossRef]
18. Puryear, W.B.; Yu, X.; Ramirez, N.P.; Reinhard, B.M.; Gummuluru, S. HIV-1 incorporation of host-cell-derived glycosphingolipid GM3 allows for capture by mature dendritic cells. *Proc. Natl. Acad. Sci. USA* **2012**, *109*, 7475–7480. [CrossRef]
19. Izquierdo-Useros, N.; Lorizate, M.; McLaren, P.J.; Telenti, A.; Kräusslich, H.-G.; Martinez-Picado, J. HIV-1 capture and transmission by dendritic cells: The role of viral glycolipids and the cellular receptor Siglec-1. *PLoS Pathog.* **2014**, *10*, e1004146. [CrossRef]
20. Akiyama, H.; Ramirez, N.-G.P.; Gudheti, M.V.; Gummuluru, S. CD169-mediated trafficking of HIV to plasma membrane invaginations in dendritic cells attenuates efficacy of anti-gp120 broadly neutralizing antibodies. *PLoS Pathog.* **2015**, *11*, e1004751. [CrossRef]

21. Hoffmann, C.; Leis, A.; Niederweis, M.; Plitzko, J.M.; Engelhardt, H. Disclosure of the mycobacterial outer membrane: Cryo-electron tomography and vitreous sections reveal the lipid bilayer structure. *Proc. Natl. Acad. Sci. USA* **2008**, *105*, 3963–3967. [CrossRef]

22. Zuber, B.; Chami, M.; Houssin, C.; Dubochet, J.; Griffiths, G.; Daffé, M. Direct visualization of the outer membrane of mycobacteria and corynebacteria in their native state. *J. Bacteriol.* **2008**, *190*, 5672–5680. [CrossRef]

23. Angala, S.K.; Belardinelli, J.M.; Huc-Claustre, E.; Wheat, W.H.; Jackson, M. The cell envelope glycoconjugates of *Mycobacterium tuberculosis*. *Crit. Rev. Biochem. Mol. Biol.* **2014**, *49*, 361–399. [CrossRef] [PubMed]

24. Bansal-Mutalik, R.; Nikaido, H. Mycobacterial outer membrane is a lipid bilayer and the inner membrane is unusually rich in diacyl phosphatidylinositol dimannosides. *Proc. Natl. Acad. Sci. USA* **2014**, *111*, 4958–4963. [CrossRef]

25. Grzegorzewicz, A.E.; de Sousa-d'Auria, C.; McNeil, M.R.; Huc-Claustre, E.; Jones, V.; Petit, C.; Angala, S.K.; Zemanová, J.; Wang, Q.; Belardinelli, J.M.; et al. Assembling of the *Mycobacterium tuberculosis* Cell Wall Core. *J. Biol. Chem.* **2016**, *291*, 18867–18879. [CrossRef]

26. Singh, P.; Rameshwaram, N.R.; Ghosh, S.; Mukhopadhyay, S. Cell envelope lipids in the pathophysiology of *Mycobacterium tuberculosis*. *Future Microbiol.* **2018**, *13*, 689–710. [CrossRef] [PubMed]

27. Barry, C.E.; Lee, R.E.; Mdluli, K.; Sampson, A.E.; Schroeder, B.G.; Slayden, R.A.; Yuan, Y. Mycolic acids: Structure, biosynthesis and physiological functions. *Prog. Lipid Res.* **1998**, *37*, 143–179. [CrossRef]

28. Dubnau, E.; Chan, J.; Raynaud, C.; Mohan, V.P.; Lanéelle, M.A.; Yu, K.; Quémard, A.; Smith, I.; Daffé, M. Oxygenated mycolic acids are necessary for virulence of *Mycobacterium tuberculosis* in mice. *Mol. Microbiol.* **2000**, *36*, 630–637. [CrossRef] [PubMed]

29. Vander Beken, S.; Al Dulayymi, J.R.; Naessens, T.; Koza, G.; Maza-Iglesias, M.; Rowles, R.; Theunissen, C.; De Medts, J.; Lanckacker, E.; Baird, M.S.; et al. Molecular structure of the *Mycobacterium tuberculosis* virulence factor, mycolic acid, determines the elicited inflammatory pattern. *Eur. J. Immunol.* **2011**, *41*, 450–460. [CrossRef]

30. Dkhar, H.K.; Nanduri, R.; Mahajan, S.; Dave, S.; Saini, A.; Somavarapu, A.K.; Arora, A.; Parkesh, R.; Thakur, K.G.; Mayilraj, S.; et al. *Mycobacterium tuberculosis* Keto-Mycolic Acid and Macrophage Nuclear Receptor TR4 Modulate Foamy Biogenesis in Granulomas: A Case of a Heterologous and Noncanonical Ligand-Receptor Pair. *J. Immunol.* **2014**, *193*, 295–305. [CrossRef] [PubMed]

31. Means, T.K.; Wang, S.; Lien, E.; Yoshimura, A.; Golenbock, D.T.; Fenton, M.J. Human toll-like receptors mediate cellular activation by *Mycobacterium tuberculosis*. *J. Immunol.* **1999**, *163*, 3920–3927.

32. Ryll, R.; Watanabe, K.; Fujiwara, N.; Takimoto, H.; Hasunuma, R.; Kumazawa, Y.; Okada, M.; Yano, I. Mycobacterial cord factor, but not sulfolipid, causes depletion of NKT cells and upregulation of CD1d1 on murine macrophages. *Microbes Infect.* **2001**, *3*, 611–619. [CrossRef]

33. Geisel, R.E.; Sakamoto, K.; Russell, D.G.; Rhoades, E.R. In vivo activity of released cell wall lipids of Mycobacterium bovis bacillus Calmette-Guérin is due principally to trehalose mycolates. *J. Immunol.* **2005**, *174*, 5007–5015. [CrossRef] [PubMed]

34. Linares, C.; Bernabéu, A.; Luquin, M.; Valero-Guillén, P.L. Cord factors from atypical mycobacteria (*Mycobacterium alvei*, *Mycobacterium brumae*) stimulate the secretion of some pro-inflammatory cytokines of relevance in tuberculosis. *Microbiology* **2012**, *158*, 2878–2885. [CrossRef] [PubMed]

35. Welsh, K.J.; Hunter, R.L.; Actor, J.K. Trehalose 6,6′-dimycolate—A coat to regulate tuberculosis immunopathogenesis. *Tuberculosis (Edinb.)* **2013**, *93*, S3–S9. [CrossRef]

36. Indrigo, J.; Hunter, R.L.; Actor, J.K. Influence of trehalose 6,6′-dimycolate (TDM) during mycobacterial infection of bone marrow macrophages. *Microbiology* **2002**, *148*, 1991–1998. [CrossRef]

37. Ishikawa, E.; Ishikawa, T.; Morita, Y.S.; Toyonaga, K.; Yamada, H.; Takeuchi, O.; Kinoshita, T.; Akira, S.; Yoshikai, Y.; Yamasaki, S. Direct recognition of the mycobacterial glycolipid, trehalose dimycolate, by C-type lectin Mincle. *J. Exp. Med.* **2009**, *206*, 2879–2888. [CrossRef]

38. Kan-Sutton, C.; Jagannath, C.; Hunter, R.L. Trehalose 6,6′-dimycolate on the surface of *Mycobacterium tuberculosis* modulates surface marker expression for antigen presentation and costimulation in murine macrophages. *Microbes Infect.* **2009**, *11*, 40–48. [CrossRef] [PubMed]

39. Hamasaki, N.; Isowa, K.; Kamada, K.; Terano, Y.; Matsumoto, T.; Arakawa, T.; Kobayashi, K.; Yano, I. In vivo administration of mycobacterial cord factor (Trehalose 6,6′-dimycolate) can induce lung and liver granulomas and thymic atrophy in rabbits. *Infect. Immun.* **2000**, *68*, 3704–3709. [CrossRef] [PubMed]

40. Sakamoto, K.; Kim, M.J.; Rhoades, E.R.; Allavena, R.E.; Ehrt, S.; Wainwright, H.C.; Russell, D.G.; Rohde, K.H. Mycobacterial trehalose dimycolate reprograms macrophage global gene expression and activates matrix metalloproteinases. *Infect. Immun.* **2013**, *81*, 764–776. [CrossRef]

41. Converse, S.E.; Mougous, J.D.; Leavell, M.D.; Leary, J.A.; Bertozzi, C.R.; Cox, J.S. MmpL8 is required for sulfolipid-1 biosynthesis and *Mycobacterium tuberculosis* virulence. *Proc. Natl. Acad. Sci. USA* **2003**, *100*, 6121–6126. [CrossRef]

42. Domenech, P.; Reed, M.B.; Dowd, C.S.; Manca, C.; Kaplan, G.; Barry, C.E. The role of MmpL8 in sulfatide biogenesis and virulence of *Mycobacterium tuberculosis*. *J. Biol. Chem.* **2004**, *279*, 21257–21265. [CrossRef]

43. Goren, M.B.; Brokl, O.; Schaefer, W.B. Lipids of putative relevance to virulence in *Mycobacterium tuberculosis*: Phthiocerol dimycocerosate and the attenuation indicator lipid. *Infect. Immun.* **1974**, *9*, 150–158. [CrossRef] [PubMed]

44. Cox, J.S.; Chen, B.; McNeil, M.; Jacobs, W.R. Complex lipid determines tissue-specific replication of *Mycobacterium tuberculosis* in mice. *Nature* **1999**, *402*, 79–83. [CrossRef]

45. Astarie-Dequeker, C.; Le Guyader, L.; Malaga, W.; Seaphanh, F.-K.; Chalut, C.; Lopez, A.; Guilhot, C. Phthiocerol dimycocerosates of *M. tuberculosis* participate in macrophage invasion by inducing changes in the organization of plasma membrane lipids. *PLoS Pathog.* **2009**, 5, e1000289. [CrossRef] [PubMed]

46. Quigley, J.; Hughitt, V.K.; Velikovsky, C.A.; Mariuzza, R.A.; El-Sayed, N.M.; Briken, V. The Cell Wall Lipid PDIM Contributes to Phagosomal Escape and Host Cell Exit of *Mycobacterium tuberculosis*. *mBio* **2017**, 8, e00148-17. [CrossRef]

47. Rousseau, C.; Winter, N.; Pivert, E.; Bordat, Y.; Neyrolles, O.; Avé, P.; Huerre, M.; Gicquel, B.; Jackson, M. Production of phthiocerol dimycocerosates protects Mycobacterium tuberculosis from the cidal activity of reactive nitrogen intermediates produced by macrophages and modulates the early immune response to infection. *Cell. Microbiol.* **2004**, 6, 277–287. [CrossRef]

48. Cambier, C.J.; Takaki, K.K.; Larson, R.P.; Hernandez, R.E.; Tobin, D.M.; Urdahl, K.B.; Cosma, C.L.; Ramakrishnan, L. Mycobacteria manipulate macrophage recruitment through coordinated use of membrane lipids. *Nature* **2014**, *505*, 218–222. [CrossRef] [PubMed]

49. Koppel, E.A.; Ludwig, I.S.; Sanchez Hernandez, M.; Lowary, T.L.; Gadikota, R.R.; Tuzikov, A.B.; Vandenbroucke-Grauls, C.M.J.E.; van Kooyk, Y.; Appelmelk, B.J.; Geijtenbeek, T.B.H. Identification of the mycobacterial carbohydrate structure that binds the C-type lectins DC-SIGN, L-SIGN and SIGNR1. *Immunobiology* **2004**, *209*, 117–127. [CrossRef]

50. Pitarque, S.; Herrmann, J.-L.; Duteyrat, J.-L.; Jackson, M.; Stewart, G.R.; Lecointe, F.; Payre, B.; Schwartz, O.; Young, D.B.; Marchal, G.; et al. Deciphering the molecular bases of *Mycobacterium tuberculosis* binding to the lectin DC-SIGN reveals an underestimated complexity. *Biochem. J.* **2005**, *392*, 615–624. [CrossRef]

51. Driessen, N.N.; Ummels, R.; Maaskant, J.J.; Gurcha, S.S.; Besra, G.S.; Ainge, G.D.; Larsen, D.S.; Painter, G.F.; Vandenbroucke-Grauls, C.M.J.E.; Geurtsen, J.; et al. Role of Phosphatidylinositol Mannosides in the Interaction between Mycobacteria and DC-SIGN. *Infect. Immun.* **2009**, *77*, 4538–4547. [CrossRef] [PubMed]

52. Vignal, C.; Guérardel, Y.; Kremer, L.; Masson, M.; Legrand, D.; Mazurier, J.; Elass, E. Lipomannans, but not lipoarabinomannans, purified from *Mycobacterium chelonae* and *Mycobacterium kansasii* induce TNF-α and IL-8 secretion by a CD14-toll-like receptor 2-dependent mechanism. *J. Immunol.* **2003**, *171*, 2014–2023. [CrossRef]

53. Quesniaux, V.J.; Nicolle, D.M.; Torres, D.; Kremer, L.; Guérardel, Y.; Nigou, J.; Puzo, G.; Erard, F.; Ryffel, B. Toll-like receptor 2 (TLR2)-dependent-positive and TLR2-independent-negative regulation of proinflammatory cytokines by mycobacterial lipomannans. *J. Immunol.* **2004**, *172*, 4425–4434. [CrossRef]

54. Gilleron, M.; Nigou, J.; Nicolle, D.; Quesniaux, V.; Puzo, G. The acylation state of mycobacterial lipomannans modulates innate immunity response through toll-like receptor 2. *Chem. Biol.* **2006**, *13*, 39–47. [CrossRef]

55. Doz, E.; Rose, S.; Nigou, J.; Gilleron, M.; Puzo, G.; Erard, F.; Ryffel, B.; Quesniaux, V.F.J. Acylation determines the toll-like receptor (TLR)-dependent positive versus TLR2-, mannose receptor-, and SIGNR1-independent negative regulation of pro-inflammatory cytokines by mycobacterial lipomannan. *J. Biol. Chem.* **2007**, *282*, 26014–26025. [CrossRef] [PubMed]

56. Puissegur, M.-P.; Lay, G.; Gilleron, M.; Botella, L.; Nigou, J.; Marrakchi, H.; Mari, B.; Duteyrat, J.-L.; Guerardel, Y.; Kremer, L.; et al. Mycobacterial lipomannan induces granuloma macrophage fusion via a TLR2-dependent, ADAM9- and β1 integrin-mediated pathway. *J. Immunol.* **2007**, *178*, 3161–3169. [CrossRef]

57. Guenin-Macé, L.; Siméone, R.; Demangel, C. Lipids of Pathogenic Mycobacteria: Contributions to Virulence and Host Immune Suppression. *Transbound. Emerg. Dis.* **2009**, *56*, 255–268. [CrossRef] [PubMed]

58. Daffé, M.; Crick, D.C.; Jackson, M. Genetics of Capsular Polysaccharides and Cell Envelope (Glyco)lipids. *Microbiol. Spectr.* **2014**, *2*, MGM2-0021-2013. [CrossRef] [PubMed]

59. Lin, Y.; Zhang, M.; Barnes, P.F. Chemokine production by a human alveolar epithelial cell line in response to *Mycobacterium tuberculosis*. *Infect. Immun.* **1998**, *66*, 1121–1126. [CrossRef] [PubMed]

60. Theus, S.A.; Cave, M.D.; Eisenach, K.D. Intracellular Macrophage Growth Rates and Cytokine Profiles of *Mycobacterium tuberculosis* Strains with Different Transmission Dynamics. *J. Infect. Dis.* **2005**, *191*, 453–460. [CrossRef] [PubMed]

61. Mvubu, N.E.; Pillay, B.; McKinnon, L.R.; Pillay, M. *Mycobacterium tuberculosis* strains induce strain-specific cytokine and chemokine response in pulmonary epithelial cells. *Cytokine* **2018**, *104*, 53–64. [CrossRef]

62. Mourik, B.C.; de Steenwinkel, J.E.M.; de Knegt, G.J.; Huizinga, R.; Verbon, A.; Ottenhoff, T.H.M.; van Soolingen, D.; Leenen, P.J.M. *Mycobacterium tuberculosis* clinical isolates of the Beijing and East-African Indian lineage induce fundamentally different host responses in mice compared to H37Rv. *Sci. Rep.* **2019**, *9*, 19922. [CrossRef]

63. Manca, C.; Reed, M.B.; Freeman, S.; Mathema, B.; Kreiswirth, B.; Barry, C.E.; Kaplan, G. Differential monocyte activation underlies strain-specific *Mycobacterium tuberculosis* pathogenesis. *Infect. Immun.* **2004**, *72*, 5511–5514. [CrossRef]

64. Reed, M.B.; Domenech, P.; Manca, C.; Su, H.; Barczak, A.K.; Kreiswirth, B.N.; Kaplan, G.; Barry, C.E. A glycolipid of hypervirulent tuberculosis strains that inhibits the innate immune response. *Nature* **2004**, *431*, 84–87. [CrossRef]

65. Tsenova, L.; Ellison, E.; Harbacheuski, R.; Moreira, A.L.; Kurepina, N.; Reed, M.B.; Mathema, B.; Barry, C.E.; Kaplan, G. Virulence of selected *Mycobacterium tuberculosis* clinical isolates in the rabbit model of meningitis is dependent on phenolic glycolipid produced by the bacilli. *J. Infect. Dis.* **2005**, *192*, 98–106. [CrossRef]

66. Theus, S.; Eisenach, K.; Fomukong, N.; Silver, R.F.; Cave, M.D. Beijing family *Mycobacterium tuberculosis* strains differ in their intracellular growth in THP-1 macrophages. *Int. J. Tuberc. Lung Dis.* **2007**, *11*, 1087–1093.

67. Akbarzadeh, A.; Rezaei-Sadabady, R.; Davaran, S.; Joo, S.W.; Zarghami, N.; Hanifehpour, Y.; Samiei, M.; Kouhi, M.; Nejati-Koshki, K. Liposome: Classification, preparation, and applications. *Nanoscale Res. Lett.* **2013**, *8*, 102. [CrossRef] [PubMed]

68. Sprott, G.D.; Dicaire, C.J.; Gurnani, K.; Sad, S.; Krishnan, L. Activation of Dendritic Cells by Liposomes Prepared from Phosphatidylinositol Mannosides from Mycobacterium bovis Bacillus Calmette-Guerin and Adjuvant Activity In Vivo. *Infect. Immun.* **2004**, *72*, 5235–5246. [CrossRef] [PubMed]

69. Rosenkrands, I.; Agger, E.M.; Olsen, A.W.; Korsholm, K.S.; Andersen, C.S.; Jensen, K.T.; Andersen, P. Cationic liposomes containing mycobacterial lipids: A new powerful Th1 adjuvant system. *Infect. Immun.* **2005**, *73*, 5817–5826. [CrossRef]

70. Cardona, P.-J. RUTI: A new chance to shorten the treatment of latent tuberculosis infection. *Tuberculosis* **2006**, *86*, 273–289. [CrossRef] [PubMed]

71. Homhuan, A.; Kogure, K.; Akaza, H.; Futaki, S.; Naka, T.; Fujita, Y.; Yano, I.; Harashima, H. New packaging method of mycobacterial cell wall using octaarginine-modified liposomes: Enhanced uptake by and immunostimulatory activity of dendritic cells. *J. Control. Release* **2007**, *120*, 60–69. [CrossRef]

72. Kawasaki, N.; Rillahan, C.D.; Cheng, T.-Y.; Van Rhijn, I.; Macauley, M.S.; Moody, D.B.; Paulson, J.C. Targeted Delivery of Mycobacterial Antigens to Human Dendritic Cells via Siglec-7 Induces Robust T Cell Activation. *J. Immunol.* **2014**, *193*, 1560–1566. [CrossRef] [PubMed]

73. Khademi, F.; Taheri, R.A.; Momtazi-Borojeni, A.A.; Farnoosh, G.; Johnston, T.P.; Sahebkar, A. Potential of Cationic Liposomes as Adjuvants/Delivery Systems for Tuberculosis Subunit Vaccines. *Rev. Physiol. Biochem. Pharmacol.* **2018**, *175*, 47–69. [CrossRef]

74. Ioerger, T.R.; Feng, Y.; Ganesula, K.; Chen, X.; Dobos, K.M.; Fortune, S.; Jacobs, W.R.; Mizrahi, V.; Parish, T.; Rubin, E.; et al. Variation among genome sequences of H37Rv strains of *Mycobacterium tuberculosis* from multiple laboratories. *J. Bacteriol.* **2010**, *192*, 3645–3653. [CrossRef]

75. Nakata, K.; Rom, W.N.; Honda, Y.; Condos, R.; Kanegasaki, S.; Cao, Y.; Weiden, M. *Mycobacterium tuberculosis* enhances human immunodeficiency virus-1 replication in the lung. *Am. J. Respir. Crit. Care Med.* **1997**, *155*, 996–1003. [CrossRef]

76. Lawn, S.D.; Pisell, T.L.; Hirsch, C.S.; Wu, M.; Butera, S.T.; Toossi, Z. Anatomically compartmentalized human immunodeficiency virus replication in HLA-DR+ cells and CD14+ macrophages at the site of pleural tuberculosis coinfection. *J. Infect. Dis.* **2001**, *184*, 1127–1133. [CrossRef]

77. McDonald, D.; Wu, L.; Bohks, S.M.; KewalRamani, V.N.; Unutmaz, D.; Hope, T.J. Recruitment of HIV and its receptors to dendritic cell-T cell junctions. *Science* **2003**, *300*, 1295–1297. [CrossRef]

78. Wu, L. Biology of HIV mucosal transmission. *Curr. Opin. HIV AIDS* **2008**, *3*, 534–540. [CrossRef]

79. Miyake, Y.; Toyonaga, K.; Mori, D.; Kakuta, S.; Hoshino, Y.; Oyamada, A.; Yamada, H.; Ono, K.-I.; Suyama, M.; Iwakura, Y.; et al. C-type lectin MCL is an FcRγ-coupled receptor that mediates the adjuvanticity of mycobacterial cord factor. *Immunity* **2013**, *38*, 1050–1062. [CrossRef]

80. Rousseau, C.; Turner, O.C.; Rush, E.; Bordat, Y.; Sirakova, T.D.; Kolattukudy, P.E.; Ritter, S.; Orme, I.M.; Gicquel, B.; Jackson, M. Sulfolipid deficiency does not affect the virulence of *Mycobacterium tuberculosis* H37Rv in mice and guinea pigs. *Infect. Immun.* **2003**, *71*, 4684–4690. [CrossRef] [PubMed]

81. Kumar, P.; Schelle, M.W.; Jain, M.; Lin, F.L.; Petzold, C.J.; Leavell, M.D.; Leary, J.A.; Cox, J.S.; Bertozzi, C.R. PapA1 and PapA2 are acyltransferases essential for the biosynthesis of the Mycobacterium tuberculosis virulence factor sulfolipid-1. *Proc. Natl. Acad. Sci. USA* **2007**, *104*, 11221–11226. [CrossRef] [PubMed]

82. Granelli-Piperno, A.; Delgado, E.; Finkel, V.; Paxton, W.; Steinman, R.M. Immature dendritic cells selectively replicate macrophagetropic (M-tropic) human immunodeficiency virus type 1, while mature cells efficiently transmit both M- and T-tropic virus to T cells. *J. Virol.* **1998**, *72*, 2733–2737. [CrossRef]

83. Sanders, R.W.; de Jong, E.C.; Baldwin, C.E.; Schuitemaker, J.H.N.; Kapsenberg, M.L.; Berkhout, B. Differential transmission of human immunodeficiency virus type 1 by distinct subsets of effector dendritic cells. *J. Virol.* **2002**, *76*, 7812–7821. [CrossRef]

84. Perot, B.P.; García-Paredes, V.; Luka, M.; Ménager, M.M. Dendritic Cell Maturation Regulates TSPAN7 Function in HIV-1 Transfer to CD4+ T Lymphocytes. *Front. Cell. Infect. Microbiol.* **2020**, *10*, 70. [CrossRef] [PubMed]

85. Bafica, A.; Scanga, C.A.; Schito, M.L.; Hieny, S.; Sher, A. Cutting Edge: In Vivo Induction of Integrated HIV-1 Expression by Mycobacteria Is Critically Dependent on Toll-Like Receptor 2. *J. Immunol.* **2003**, *171*, 1123–1127. [CrossRef]

86. Equils, O.; Schito, M.L.; Karahashi, H.; Madak, Z.; Yarali, A.; Michelsen, K.S.; Sher, A.; Arditi, M. Toll-Like Receptor 2 (TLR2) and TLR9 Signaling Results in HIV-Long Terminal Repeat Trans-Activation and HIV Replication in HIV-1 Transgenic Mouse Spleen Cells: Implications of Simultaneous Activation of TLRs on HIV Replication. *J. Immunol.* **2003**, *170*, 5159–5164. [CrossRef] [PubMed]

87. Larson, E.C.; Novis, C.L.; Martins, L.J.; Macedo, A.B.; Kimball, K.E.; Bosque, A.; Planelles, V.; Barrows, L.R. *Mycobacterium tuberculosis* reactivates latent HIV-1 in T cells in vitro. *PLoS ONE* **2017**, *12*, e0185162. [CrossRef] [PubMed]

88. Goletti, D.; Weissman, D.; Jackson, R.W.; Collins, F.; Kinter, A.; Fauci, A.S. The in vitro induction of human immunodeficiency virus (HIV) replication in purified protein derivative-positive HIV-infected persons by recall antigen response to *Mycobacterium tuberculosis* is the result of a balance of the effects of endogenous interleu. *J. Infect. Dis.* **1998**, *177*, 1332–1338. [CrossRef] [PubMed]

89. Hoshino, Y.; Tse, D.B.; Rochford, G.; Prabhakar, S.; Hoshino, S.; Chitkara, N.; Kuwabara, K.; Ching, E.; Raju, B.; Gold, J.A.; et al. *Mycobacterium tuberculosis*-induced CXCR4 and chemokine expression leads to preferential X4 HIV-1 replication in human macrophages. *J. Immunol.* **2004**, *172*, 6251–6258. [CrossRef] [PubMed]

90. Rodriguez, M.E.; Loyd, C.M.; Ding, X.; Karim, A.F.; McDonald, D.J.; Canaday, D.H.; Rojas, R.E. Mycobacterial phosphatidylinositol mannoside 6 (PIM6) up-regulates TCR-triggered HIV-1 replication in CD4+ T cells. *PLoS ONE* **2013**, *8*, e80938. [CrossRef]

91. Tomlinson, G.S.; Bell, L.C.K.; Walker, N.F.; Tsang, J.; Brown, J.S.; Breen, R.; Lipman, M.; Katz, D.R.; Miller, R.F.; Chain, B.M.; et al. HIV-1 infection of macrophages dysregulates innate immune responses to *Mycobacterium tuberculosis* by inhibition of interleukin-10. *J. Infect. Dis.* **2014**, *209*, 1055–1065. [CrossRef]

92. Bhatt, K.; Gurcha, S.S.; Bhatt, A.; Besra, G.S.; Jacobs, W.R. Two polyketide-synthase-associated acyltransferases are required for sulfolipid biosynthesis in *Mycobacterium tuberculosis*. *Microbiology* **2007**, *153*, 513–520. [CrossRef] [PubMed]

93. Dobson, G.; Minnikin, D.E.; Minnikin, S.M.; Parlett, J.H.; Goodfellow, M.; Ridell, M.; Magnusson, M. Systematic analysis of complex mycobacterial lipids. In *Chemical Methodscin Bacterial Systematics*; Goodfellow, M., Minnikin, D.E., Eds.; Academic Press: London, UK, 1985; Volume 1, pp. 237–265.